Cell Reports
Medicine

Article

Vaccine-induced ICOS^{+}CD38^{+} circulating Tfh are sensitive biosensors of age-related changes in inflammatory pathways

Graphical abstract

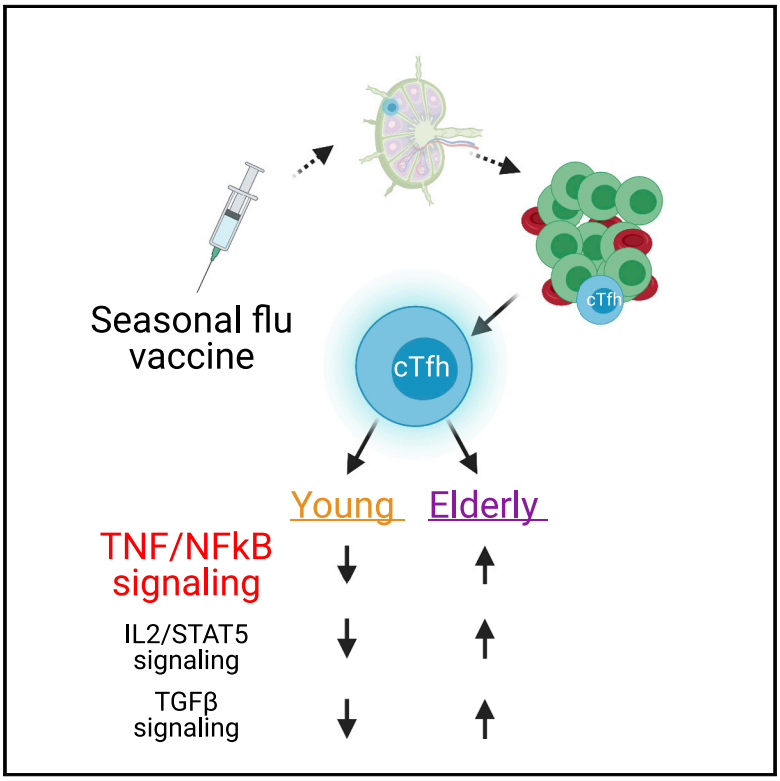

Highlights

- Vaccine-induced ICOS^{+}CD38^{+} cTfh show increased TNF-NF-κB signaling with aging
- TNF-NF-κB signaling is beneficial for cTfh survival in the elderly
- Vaccine-induced cTfh are sensors of background changes in immune environment

Authors

Ramin Sedaghat Herati, Luisa Victoria Silva, Laura A. Vella, ..., Hildegund C.J. Ertl, Kenneth E. Schmader, E. John Wherry

Correspondence

ramin.herati@nyulangone.org (R.S.H.), wherry@pennmedicine.upenn.edu (E.J.W.)

In brief

A better understanding of T follicular helper (Tfh) CD4 cells may lead to improved vaccine design. Herati et al. identify altered NF-κB signaling with aging in the transcriptional profiles of vaccine-induced circulating Tfh responses after influenza vaccine and demonstrate the use of these cells as cellular biosensors of the underlying immune state.

Herati et al., 2021, Cell Reports Medicine 2, 100262
May 18, 2021
https://doi.org/10.1016/j.xcrm.2021.100262

CellPress

Cell Reports Medicine

CellPress
OPEN ACCESS

Article

Vaccine-induced ICOS$^+$CD38$^+$ circulating Tfh are sensitive biosensors of age-related changes in inflammatory pathways

Ramin Sedaghat Herati,[1,2,13,*] Luisa Victoria Silva,[3] Laura A. Vella,[3,4] Alexander Muselman,[5] Cecile Alanio,[3,6] Bertram Bengsch,[7] Raj K. Kurupati,[8] Senthil Kannan,[8] Sasikanth Manne,[3,6] Andrew V. Kossenkov,[8] David H. Canaday,[9,10] Susan A. Doyle,[11,12] Hildegund C.J. Ertl,[8] Kenneth E. Schmader,[11,12] and E. John Wherry[3,6,*]

[1]Division of Infectious Diseases and Immunology, Department of Medicine, New York University School of Medicine, New York, NY 10016, USA
[2]Department of Microbiology, New York University School of Medicine, New York, NY, USA
[3]Institute for Immunology, University of Pennsylvania Perelman School of Medicine, Philadelphia, PA, USA
[4]Department of Medicine, Children's Hospital of Philadelphia, Philadelphia, PA 19104, USA
[5]Department of Immunology, Stanford University, Stanford, CA 94305, USA
[6]Department of Systems Pharmacology and Translational Therapeutics, University of Pennsylvania Perelman School of Medicine, Philadelphia, PA 19104, USA
[7]Department of Internal Medicine II, University Medical Center Freiburg, and Signalling Research Centres BIOSS and CIBSS, University of Freiburg, Freiburg, Germany
[8]Wistar Institute, Philadelphia, PA 19104, USA
[9]Division of Infectious Disease, Case Western Reserve University, Cleveland, OH, USA
[10]Geriatric Research, Education, and Clinical Center, Cleveland VA Medical Center, Cleveland, OH, 44195, USA
[11]Division of Geriatrics, Department of Medicine, Duke University Medical Center, Durham, NC, USA
[12]Geriatric Research, Education, and Clinical Center, Durham VA Medical Center, Durham, NC 27710, USA
[13]Lead contact
*Correspondence: ramin.herati@nyulangone.org (R.S.H.), wherry@pennmedicine.upenn.edu (E.J.W.)
https://doi.org/10.1016/j.xcrm.2021.100262

SUMMARY

Humoral immune responses are dysregulated with aging, but the cellular and molecular pathways involved remain incompletely understood. In particular, little is known about the effects of aging on T follicular helper (Tfh) CD4 cells, the key cells that provide help to B cells for effective humoral immunity. We performed transcriptional profiling and cellular analysis on circulating Tfh before and after influenza vaccination in young and elderly adults. First, whole-blood transcriptional profiling shows that ICOS$^+$CD38$^+$ cTfh following vaccination preferentially enriches in gene sets associated with youth versus aging compared to other circulating T cell types. Second, vaccine-induced ICOS$^+$CD38$^+$ cTfh from the elderly had increased the expression of genes associated with inflammation, including tumor necrosis factor-nuclear factor κB (TNF-NF-κB) pathway activation. Finally, vaccine-induced ICOS$^+$CD38$^+$ cTfh display strong enrichment for signatures of underlying age-associated biological changes. These data highlight the ability to use vaccine-induced cTfh as cellular "biosensors" of underlying inflammatory and/or overall immune health.

INTRODUCTION

Influenza vaccination induces strain-specific neutralizing antibodies in healthy adults, but this process is impaired with aging.[1–4] Moreover, immunological aging, which may or may not be directly linked to chronological aging, is associated with increased morbidity and mortality from infectious diseases.[5–7] Studies of immunological aging and vaccines have identified mechanisms, including alterations at the subcellular,[8–11] cellular,[12,13] and systems levels,[14–17] that lead to altered vaccine responses. Vaccination strategies that effectively overcome age-associated immune dysfunction are of great interest for rational vaccine design.

The production of class-switched, affinity-matured antibody by B cells is dependent on help from T follicular helper (Tfh) cells in germinal centers (GCs) in lymphoid tissues,[18] but few studies have evaluated the effects of aging on the GC reaction and GC-dependent cellular responses in humans. Suboptimal vaccine responses with aging have been associated with alterations in cellular pathways, such as tumor necrosis factor-nuclear factor-κB (TNF-NF-κB).[19] For example, several studies observed a modest negative correlation between serum TNF and vaccine responses.[12,20–22] However, therapeutic anti-TNF antibody paradoxically did not result in improved humoral responses and instead led to reduced vaccine-induced antibody responses to pneumococcal and influenza vaccines.[23–25] Furthermore,

mice deficient in TNF receptor 1 or TNF failed to make GCs and were unable to mount sustained immunoglobulin G (IgG) responses to immunization.[26–29] Thus, the role of TNF signaling in GC and Tfh responses remains poorly understood, but it is likely to be critically important.[30–32] Understanding age-associated alterations in pathways such as TNF and others[13,16,33,34] will be necessary for designing effective vaccines for the elderly.

In humans, directly studying the events leading to productive humoral immunity is challenging because lymphoid tissue is not readily available after vaccination. Several studies have examined a subset of CD4 T cells in human peripheral blood, called circulating T follicular helper cells (cTfh), that possesses phenotypic, transcriptional, and functional similarities to lymphoid Tfh.[35–40] Some features of cTfh likely reflect events in lymphoid tissue. For example, vaccine-induced changes in cTfh correlate with changes in influenza-specific antibody production.[38–40] The subset of cTfh expressing high ICOS and CD38 is expanded in blood 7 days after influenza vaccination, correlates with the plasmablast response, and includes recurring influenza-specific T cell receptor clonotypes each year after influenza vaccination.[41] Moreover, we recently demonstrated that ICOS$^+$CD38$^+$ cTfh can be found in lymph and share characteristic features of GC-Tfh.[42] Thus, cTfh may be useful as a cellular biomarker of immunological events, including vaccination, and possibly the broader state of lymphoid compartments from which these cells recently emerged. Moreover, profiling cTfh may provide opportunities to identify the underlying reasons for suboptimal vaccine responses in human populations, including the elderly.

Here, we tested the effects of aging on cTfh after influenza vaccination. Transcriptional profiling of cTfh subsets responding to vaccination revealed key age-associated pathway-level differences in cTfh responses to influenza vaccination. In particular, transcriptional signatures downstream of TNF-NF-κB signaling pathway were enriched in responding ICOS$^+$CD38$^+$ cTfh from elderly adults compared to young adults at 7 days after vaccination. This transcriptional program was associated with a pro-survival effects in these ICOS$^+$CD38$^+$ cTfh. Focusing on activated cTfh responding to vaccination also revealed additional age-related inflammatory pathway differences. In particular, on day 7 after vaccination, ICOS$^+$CD38$^+$ cTfh from older adults displayed transcriptional evidence of major alterations in interleukin-2-signal transducer and activator of transcription 5 (IL-2-STAT5) signaling, IL-6-STAT3 signaling, and other pathways. When examined for general signatures of aging versus youth, ICOS$^+$CD38$^+$ cTfh enriched far better for these signatures than other blood T cell types, suggesting that vaccine-induced or recently activated cTfh are sensitive biomarkers of underlying changes in immune fitness. Thus, these studies identify key changes in cTfh with age that may relate to altered humoral immunity following vaccination.

RESULTS

ICOS$^+$CD38$^+$ cTfh response appears similar with aging

Antibody responses to vaccination depend on Tfh help to B cells,[43] but the effects of aging on Tfh responses remain poorly understood. We and others have demonstrated that blood cTfh can provide insights into Tfh biology relevant to vaccine responses.[38–41] The subset of cTfh expressing ICOS and CD38 are highly activated, expand after influenza vaccination, and contain the influenza-specific clonotypes[38,41]; moreover, activated Tfh similar to those in the blood can be found in lymph and have characteristics similar to GC-Tfh, suggesting a direct relationship between ICOS$^+$CD38$^+$ cTfh and events in lymphoid tissue.[42] Here, we focused on this ICOS$^+$CD38$^+$ cTfh subset to understand age-related changes in vaccine-induced immunity.

Our previous work revealed an age-related decrease in total cTfh, defined as CD4$^+$CXCR5$^+$PD-1$^+$ T cells in the blood, but whether there were differences in the more activated, vaccine-responding cTfh cells expressing ICOS together with CD38 and/or Ki67 was less clear.[38] Thus, because the ICOS$^+$CD38$^+$ cTfh subset contains vaccine-responding T cell clones, we sought to investigate this population in more detail in young and elderly adults (Table S1). We again defined cTfh as non-naive CD4$^+$CXCR5$^+$PD-1$^+$ T cells (Figure S1A).[38,41] Similar to our previous findings,[38] elderly adults had a 19% lower frequency of total CXCR5$^+$PD-1$^+$ cTfh in circulation and a 1.2-fold higher expression of ICOS at baseline ($p = 0.05$ and $p = 0.06$, respectively; Figures S1B and S1C). However, among cTfh, the frequency of cells expressing ICOS and CD38 was similar in young and elderly at baseline (Figures 1A and S1D) and after influenza vaccination (Figures 1B, 1C, and S1E). The vaccine-induced increase in PD-1 expression was also comparable in both cohorts for the ICOS$^+$CD38$^+$ cTfh population (Figures 1D and S1F). In line with the role of Tfh providing help to B cells, the vaccine-induced fold change in the ICOS$^+$CD38$^+$ cTfh response correlated with the vaccine-induced fold change in the plasmablast response but was not different with aging (young, Pearson $r = 0.57$, $p = 3.9 \times 10^{-3}$; elderly, Pearson $r = 0.67$, $p = 4.8 \times 10^{-4}$) (Figures 1E and S1G). Thus, the magnitude of the influenza vaccine-induced cTfh responses and their correlation with the plasmablast response was similar in young and elderly adults.

We next hypothesized that transcriptional profiling may be more sensitive than flow cytometric analysis for revealing differences in cTfh responses. We performed RNA sequencing (RNA-seq) on ICOS$^+$CD38$^+$ cTfh, ICOS$^-$CD38$^-$ cTfh, and naive CD4$^+$ cells from young ($n = 6$) and elderly ($n = 8$) adults before and after influenza vaccination (Figures S1H–S1J). In both age groups, ICOS$^+$CD38$^+$ cTfh had a distinct transcriptomic signature, with a higher expression of genes previously described in Tfh,[18,44–46] such as *MAF*, *BCL6*, and *TIGIT*, compared to naive CD4, and ICOS$^+$CD38$^+$ cTfh expressed more *CD38*, *MKI67*, and *POU2AF1* than ICOS$^-$CD38$^-$ cTfh (Figures 1F and S1K). Moreover, the ICOS$^+$CD38$^+$ cTfh displayed greater similarity to lymphoid GC-Tfh than the ICOS$^-$CD38$^-$ cTfh subset by gene set enrichment analyses (GSEAs)[47] for human tonsillar GC-Tfh[36] and mouse lymphoid GC-Tfh[48,49] datasets (Figures S1L–S1N; Table S2), irrespective of aging. In general, however, although the three CD4 T cell populations examined had distinct transcriptional profiles, the age-related differences within each of these cell types at the level of individual genes, such as *POU2AF1*, were minimal (Figures 1F and S1O). Thus, the ICOS$^+$CD38$^+$ cTfh response to influenza vaccination was similar in young versus elderly adults, at least at this level of resolution.

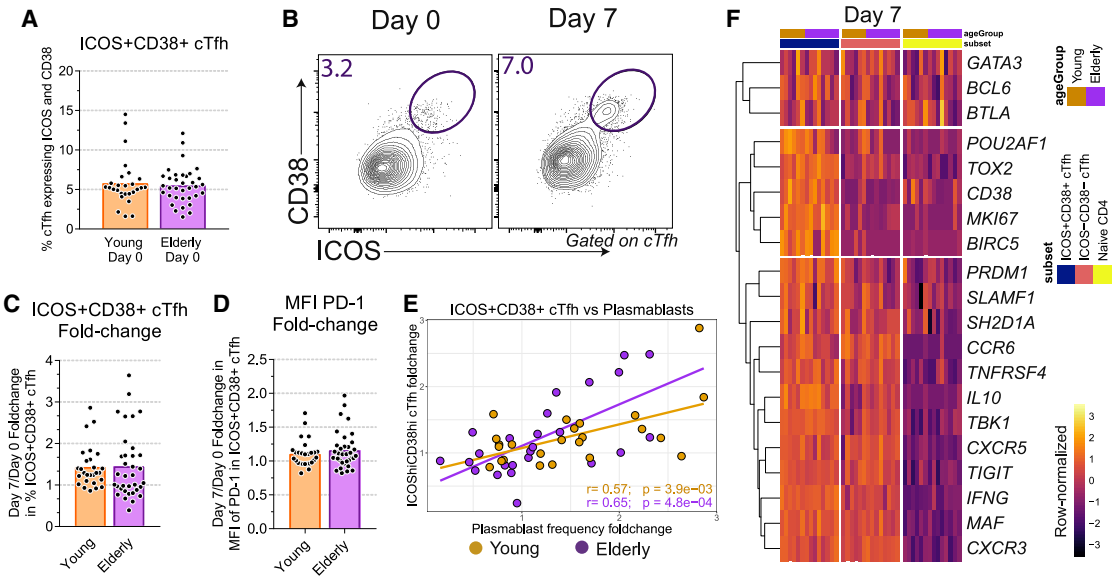

Figure 1. ICOS$^+$CD38$^+$ cTfh responses appear similar with aging

A cohort of young adults (n = 28) and elderly adults (n = 35) received influenza vaccination in Fall 2014.

(A and B) Flow cytometry for days 0 and 7 after vaccination in the frequency of cTfh co-expressing ICOS and CD38 for young (orange, n = 27) and elderly (purple, n = 35) adults.

(C and D) Fold change between days 0 and 7 for the change in ICOS$^+$CD38$^+$ cTfh frequency (C) or geometric MFI of PD-1 (D) in ICOS$^+$CD38$^+$ cTfh for young (orange, n = 27) and elderly (purple, n = 35) adults.

(E) Correlation between ICOS$^+$CD38$^+$ cTfh frequency fold change at day 7 compared to day 0, and the plasmablast fold change at day 7 compared to day 0 for young (orange, n = 25) and elderly (purple, n = 26) adults.

(F) Peripheral blood mononuclear cells (PBMCs) from young (n = 6) and elderly (n = 8) adults were sorted for ICOS$^+$CD38$^+$ cTfh, ICOS$^-$CD38$^-$ cTfh, and naive CD4 at days 0 and 7 after vaccination. Log-transformed transcriptional profiling data were queried for selected genes for young (orange) and elderly (purple) adults at day 7 after vaccination. The heatmap is row normalized.

TNF-NF-κB signaling is enriched with aging in ICOS$^+$CD38$^+$ cTfh

Despite the findings above, previous studies have suggested that cTfh from older adults may differ qualitatively or functionally from those in younger adults.[3,13,34] To further interrogate the question of age-related differences in the cTfh response to vaccination, we directly compared the transcriptional profiles of ICOS$^+$CD38$^+$ cTfh from young and elderly adults at day 7 (Figure 2A), when the ICOS$^+$CD38$^+$ cTfh population in blood is enriched for influenza-specific cells.[41] Transcriptional differences were revealed for ICOS$^+$CD38$^+$ cTfh from young compared to elderly adults at day 7 (Figures S2A and S2B). Differentially expressed genes included *PLCG2*, *RNF130*, *RAB2A*, and *ACSL3*, which were increased in cTfh from elderly adults, whereas *CD27*, *CD6*, *EIF1AD*, *EEF2*, and *MAP2K2* were increased in the young (Figure S2C). CD27, a member of the TNF receptor family, was more strongly expressed at the protein level in the ICOS$^+$CD38$^+$ cTfh from young adults compared to elderly adults (Figure S2D). Overall, however, examining differences in the expression of individual genes did not reveal obvious age-related changes (Figures S1J, S1K, S2A, and S2B) that would explain differences in vaccination outcomes with age, suggesting that differences in cTfh between young and older adults, if they existed, may reside in the coordination of the transcriptional programs.

We, therefore, next hypothesized that there may be broader age-related differences at the pathway level. GSEA identified multiple gene sets potentially relevant to age-related biological changes that preferentially enriched in the ICOS$^+$CD38$^+$ cTfh from the elderly adults compared to young ICOS$^+$CD38$^+$ cTfh at day 7 post-vaccination (Figure S2E). For example, the IL-2/STAT5 signaling pathway was previously demonstrated to have an inhibitory effect on Tfh differentiation via Blimp-1.[50] There was stronger enrichment for the IL-2/STAT5 signaling pathway in ICOS$^+$CD38$^+$ cTfh from the elderly adults (Figure S2E), although this enrichment did not correspond to detectable differences in *PRDM1* transcripts in the blood (Figure 1F). Among the inflammatory signatures with the greatest enrichment in the ICOS$^+$CD38$^+$ cTfh from the elderly adults was TNF-NF-κB signaling (Figure S2E). These enrichment patterns were biased to pathway enrichment in ICOS$^+$CD38$^+$ cTfh from elderly adults, with no specific gene sets enriched in ICOS$^+$CD38$^+$ cTfh from the young adults even at a more relaxed false discovery rate (FDR) of <0.20, thereby suggesting more distinct biological changes in the elderly. These data highlighted the potential differential use or engagement of the NF-κB signaling pathway by ICOS$^+$CD38$^+$ cTfh in elderly adults compared to young adults at day 7 post-vaccination.

These observations provoked the hypothesis that inflammatory signals could result in transcriptional network differences in the vaccine-induced cTfh from elderly adults. To investigate this possibility, we next applied weighted gene correlation network analysis (WGCNA)[51] to more deeply interrogate the underlying transcriptional networks of vaccine-induced cTfh from

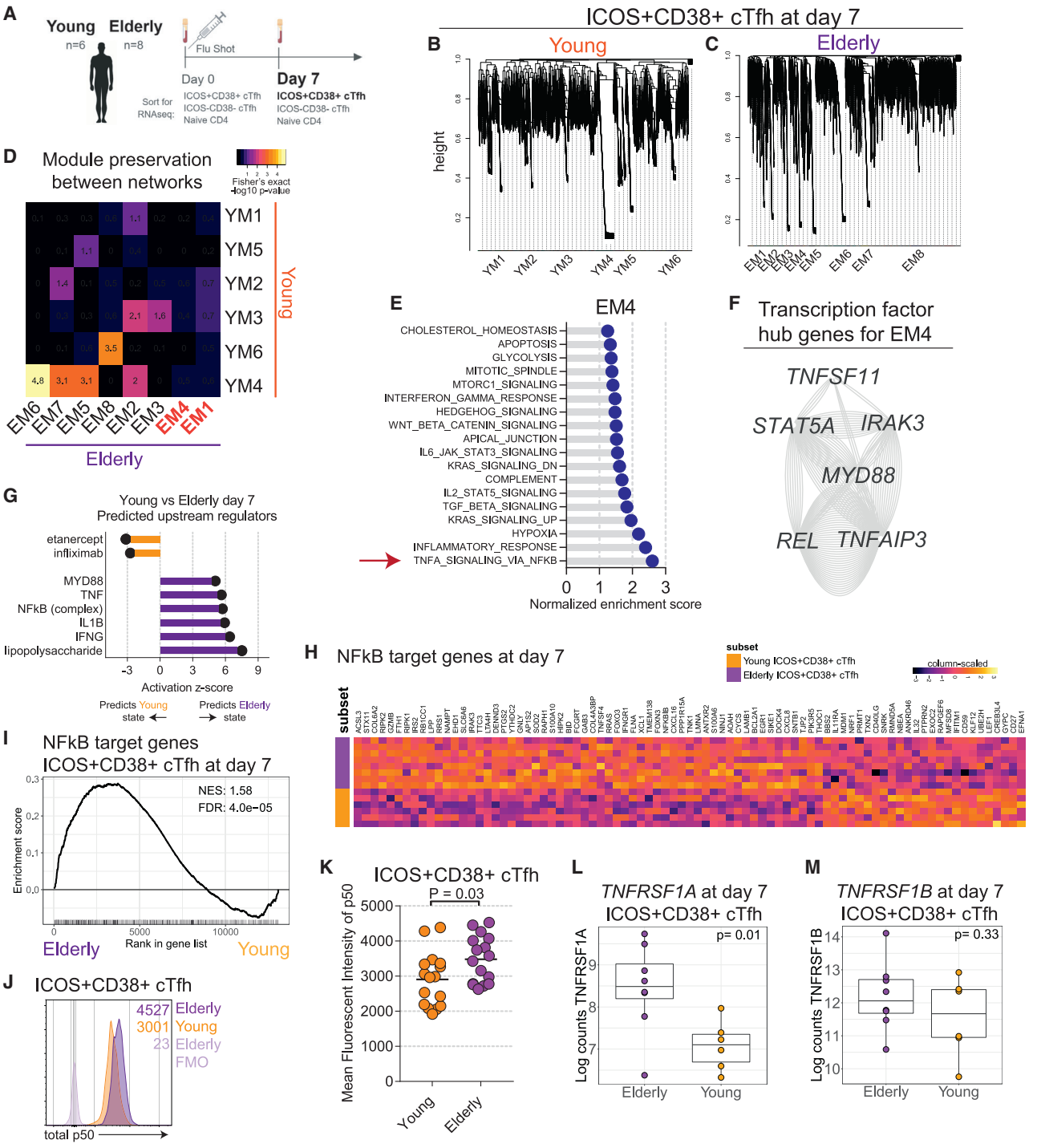

Figure 2. TNF-NF-κB pathway is enriched with aging in ICOS$^+$CD38$^+$ cTfh

(A) Schematic for RNA-seq analyses.

(B and C) Weighted gene correlation network analysis on ICOS$^+$CD38$^+$ cTfh at day 7 from young (B) and elderly (C) adults.

(D) Module preservation analysis was performed using Fisher's exact test. Heatmap color and value indicate the $-\log_{10}$(p value) for the overlap in genes in modules.

(E) Genes ranked based on module membership for elderly module EM4. Then, GSEA was performed using the MSigDB HALLMARK collection. Positive enrichment scores indicate enrichment for genes in EM4.

(F) Transcription factors with module membership >0.80 in EM4 displayed as a multiple association network (GeneMANIA without gene prediction).

(G) Ingenuity Pathway Analysis for predicted upstream regulators for ICOS$^+$CD38$^+$ cTfh at day 7 for young and elderly adults.

(legend continued on next page)

young versus elderly. An advantage of WGCNA is the ability to identify biologically meaningful groups of co-varying genes, even if the individual genes are not statistically differentially expressed. Taking advantage of co-variance often identifies major changes in biological circuits that are not apparent at the level of individual genes. At day 7 after vaccination, 6 transcriptional modules were identified for the ICOS$^+$CD38$^+$ cTfh subset isolated from young adults, whereas 8 transcriptional modules were identified from the elderly (Figures 2B, 2C, S2F, and S2G; Table S3). Although most modules in young adults overlapped with $\geq$1 modules in the elderly, 2 modules in the elderly (EM1 and EM4) did not have significant overlap with any module in young adults (Figure 2D). To evaluate the underlying biology of these modules, we used GSEA on genes ranked by module membership (Figures 2E and S2H), which revealed TNF-NF-κB signaling to be the highest-scoring pathway associated with EM4. After filtering the EM4 gene list for transcription factors,[52] we identified a dense network of six hub genes—*IRAK3*, *MYD88*, *TNFAIP3*, *STAT5A*, *REL*, and *TNFSF11*—that had direct relevance to the NF-κB signaling pathway (Figures 2F and S2I; Table S4). In addition, Ingenuity Pathway Analysis (IPA) for upstream regulators[53,54] predicted lipopolysaccharides (LPS), IL-1B, NF-κB (complex), TNF, and MYD88 to be more activated in ICOS$^+$CD38$^+$ cTfh from elderly adults compared to young adults at day 7 following vaccination, and signatures associated with blocking TNF signaling biased in the opposite direction (Figures 2G and S2J). In addition, several other inflammatory pathways were strongly enriched in EM4, including inflammatory response, transforming growth factor β (TGF-β) signaling, IL-2 STAT5 signaling, and IL-6 JAK STAT3 signaling, as were signatures of hypoxia and complement (Figure 2E). Module EM1 also enriched for inflammatory pathways with type I and type II interferon pathways as the strongest signatures (Figure S2H). These results identified coordinated transcriptional changes reflecting inflammatory signaling in the elderly.

We next asked whether genes downstream of NF-κB were affected, using a list of ~1,500 NF-κB target genes.[55] We identified 58 targets of NF-κB that were upregulated in ICOS$^+$CD38$^+$ cTfh at day 7 in elderly adults compared with 25 that were upregulated in young adults at Padj < 0.05 (Figures 2H and S2K). GSEA also identified stronger enrichment of the gene targets of NF-κB in the ICOS$^+$CD38$^+$ cTfh at day 7 from elderly compared to young adults (Figure 2I). These data support the observation of increased inflammatory signaling in ICOS$^+$CD38$^+$ cTfh with aging.

Circulating inflammatory cytokines can differ in elderly compared to young adults,[56] which is consistent with the notion of immune dysregulation and chronic inflammation during aging.[15,57] At baseline, we identified higher levels of TNF, C-X-C motif chemokine 11 (CXCL11), and macrophage inflammatory protein 1β (MIP1β) in the plasma of elderly compared to young adults (Figure S2L). We then used gene set variation analysis (GSVA)[58] to investigate whether the plasma TNF concentrations had any relationship to the increase in the TNF-NF-κB gene set signature in ICOS$^+$CD38$^+$ cTfh from elderly adults at 7 days after immunization, but we found no correlation (Figures S3A and S3B). These data suggested that serum TNF alone was unlikely to be the sole cause of the observed TNF-NF-κB transcriptional signature.

To further investigate a potential role for differences in NF-κB signaling, we next tested whether there was evidence for constitutive upregulation and/or activation of the NF-κB pathway *ex vivo*. NF-κB1 (p50) protein expression was elevated in ICOS$^+$CD38$^+$ cTfh from elderly adults compared to young adults (Figures 2J, 2K, S3C, and S3D) suggesting the greater activation of, or the ability to activate, this pathway in response to inflammatory mediators in the ICOS$^+$CD38$^+$ cTfh from aged individuals. TNF signaling occurs via the interaction of soluble or membrane-bound TNF with TNF receptors CD120a and CD120b (TNFR1 and TNFR2, respectively), with soluble TNF signaling more strongly through TNFR1 than TNFR2.[59] To test whether cTfh differentially expressed TNFR1 or TNFR2, transcriptional profiling data for CD4 T cell subsets was evaluated for TNFR1 (gene name *TNFRSF1A*) and TNFR2 (gene name *TNFRSF1B*). ICOS$^+$CD38$^+$ cTfh had higher gene expression for TNFR1 and TNFR2 than other CD4 subsets at baseline (Figure S3E). Following vaccination, *TNFRSF1A* expression in ICOS$^+$CD38$^+$ cTfh was increased in elderly compared to young adults, although the expression of *TNFRSF1B* was similar (Figures 2L, 2M, and S3F–S3H). Thus, several components of the TNF signaling pathway are elevated in vaccine-induced ICOS$^+$CD38$^+$ cTfh from elderly compared to young adults.

TNF signaling promotes Tfh-B cell interactions

TNF-NF-κB signaling with aging has been associated with age-related immune dysfunction.[57] Our transcriptional and network analyses highlighted a role for increased NF-κB signaling with aging within ICOS$^+$CD38$^+$ cTfh at day 7 post-vaccination. We hypothesized that TNF-NF-κB signaling may adversely affect Tfh-B cell interactions. To test this idea, we used cTfh-B cell coculture using autologous naive B cells and CD4 T cells from young adults to interrogate pathways involved in cTfh provision of help to B cells *in vitro*.[35–38] As expected, cTfh (defined as non-naive CD4$^+$CXCR5$^+$PD-1$^+$) were the major supplier of B cell help, as evidenced by higher IgM and IgG1 in supernatant after staphylococcal enterotoxin B (SEB) stimulation compared to controls (Figures 3A and 3B). To test the impact of TNF on the ability of cTfh to provide help, recombinant TNF protein or α-TNF antibody was added at the beginning of the coculture. Adding TNF did not augment B cell help and antibody production compared to SEB alone (Figures 3A and 3B). In contrast, the addition of α-TNF blocking antibodies reduced supernatant IgG1 concentrations

(H) Differentially expressed NF-κB target genes comparing ICOS$^+$CD38$^+$ cTfh at day 7 from elderly (purple) and young (orange) adults.
(I) GSEA for NF-κB target genes to compare ICOS$^+$CD38$^+$ cTfh from elderly and young adults.
(J) Example plot from 1 young adult and 1 elderly adult for total NF-κB p50 protein from an independent cohort of young and elderly adults. Geometric mean fluorescence intensity (MFI) shown.
(K) Total NF-κB p50 for ICOS$^+$CD38$^+$ cTfh at baseline in young (orange) and elderly (purple) adults (n = 16 in each group), as taken from an independent cohort of young and elderly adults.
(L and M) Gene expression for *TNFRSF1A* (L) (n = 6 for young; n = 8 for elderly) and *TNFRSF1B* (M) (n = 8 for elderly) shown at day 7 after vaccine from $\log_2$-transformed counts data for young (orange) and elderly (purple) adults.

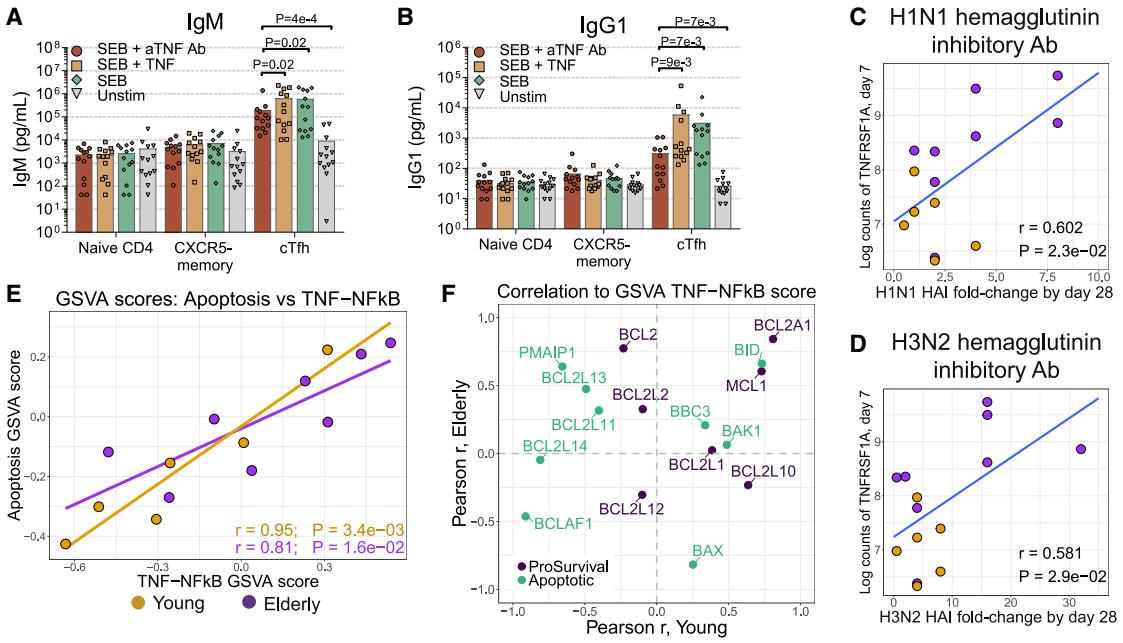

Figure 3. TNF signaling promotes Tfh-B cell interactions

(A and B) PBMC from young adults were freshly isolated and sorted for coculture of T cell subsets (naive, gated as $CD4^+CD45RA^+CD27^+$; $CXCR5^-$ memory, non-naive $CD4^+CXCR5^-$; cTfh, non-naive $CD4^+CXCR5^+PD\text{-}1^+$) with autologous naive B cells ($CD3^-CD19^+CD27^{lo}IgD^+$). Supernatant IgM (A) and IgG1 (B) were measured after 7 days, as shown for the following conditions: unstimulated (gray), SEB alone (0.5 μg/mL, green), SEB with recombinant human TNF (125 ng/mL, tan), or SEB with α-TNF antibodies (2 μg/mL, sienna) (1-way repeated-measures ANOVA with Holm-Sidak's test; n = 12 per group).

(C and D) Correlation shown for the *TNFRSF1A* in $ICOS^+CD38^+$ cTfh at day 7 compared with the H1N1-specific (C) hemagglutinin inhibitory (HAI) titer (n = 14) or H3N2-specific (D) HAI titer (n = 14) in young (orange) and elderly (purple) adults.

(E) Correlation of apoptosis and NF-κB gene set GSVA scores for $ICOS^+CD38^+$ cTfh at day 7 for young (orange, n = 6) and elderly (purple, n = 8) adults.

(F) Pearson coefficients for BCL family member genes compared to GSVA scores for TNF-NF-κB signaling in $ICOS^+CD38^+$ cTfh at day 7 for young (x axis) and elderly (y axis) adults. Genes classified as either pro-survival (dark blue) or apoptotic (sea green).

10-fold compared to SEB alone (Figure 3B). The differentiation of naive B cells into $CD19^+CD38^+CD20^{lo}$ plasmablasts was reduced in the presence of α-TNF antibodies, but the addition of TNF also had no effect (Figure S4A). IgG1 production by naive B cells stimulated *in vitro* with α-IgM and soluble trimeric CD40L did not change upon the addition of α-TNF antibodies (Figure S4B), suggesting that reduced antibody production by B cells in the context of the blockade of TNF signaling in the presence of cTfh was through the effects of TNF signaling on Tfh. Live cell counts for T and B cells decreased when α-TNF antibodies were added to the cocultures (Figure S4C) or when the TNF-converting enzyme inhibitor TAPI-0[60] was used (Figure S4D), suggesting a potential pro-survival role for TNF signaling. Although nonspecific effects of α-TNF antibodies in these cultures are possible, the decreased survival observed with increasing concentrations of TAPI-0 also support a role for soluble TNF signaling. These studies only addressed whether TNF signals could play a role in the Tfh provision of help to B cells in general, but they did not address the question of aging because of potential age-related confounders in the autologous naive B cell compartment from elderly adults.[61] To further explore the role of TNF in cTfh biology in the setting of aging, TNF was assessed in supernatants from previously performed cocultures[38] in which $CD4^+CXCR5^+PD\text{-}1^+$ cells were cocultured at a 1:1 ratio with allogenic naive B cells from a common young donor, thereby allowing the biology of cTfh from older donors to be assessed *in vitro*. We found a correlation between age and TNF in the supernatant after 7 days of coculture (Figure S4E; Pearson r = 0.35, p = 0.048). Because these cocultures used the same source of naive allogeneic B cells from a single young donor, the greater production of TNF was likely due to cTfh from the elderly adults. These data indicated an age-associated upregulation of the NF-κB signaling pathway in the $ICOS^+CD38^+$ cTfh after vaccination that was associated with increased TNF production during Tfh-B cell interactions in the elderly. Moreover, these data suggested a role for TNF-NF-κB signaling in promoting cellular survival in the context of Tfh-B cell interactions.

Given the coculture data, we hypothesized that TNF-NF-κB signaling may be associated with a beneficial effect on the humoral response *in vivo*. Influenza vaccination was associated with the higher expression of *TNFRSF1A* in $ICOS^+CD38^+$ cTfh in elderly adults compared to young adults following vaccination (Figures 2L and 2M). Thus, we next compared the expression of *TNFRSF1A* and *TNFRSF1B* to the neutralizing antibody responses. Both young and elderly adults produced influenza strain-specific binding antibodies and had high neutralizing antibody titers following vaccination (Figures S4F and S4G). Examining young and elderly adults together, *TNFRSF1A* expression by $ICOS^+CD38^+$ cTfh (but not other CD4 subsets) positively correlated with the fold change in the strain-specific neutralizing

antibody titers at day 28 compared to day 0 (Figures 3C, 3D, and S4H). These data support the notion of a positive role for TNF-NF-κB signaling in Tfh-B cell interactions. Moreover, these observations are consistent with observations that clinical TNF blockade resulted in reduced vaccine immunogenicity.[23,24]

Since TNF blockade was associated with reduced survival of cTfh and B cells in cocultures *in vitro*, we next asked whether there was an association between TNF signaling and cell death *in vivo*. GSVA scores for TNF-NF-κB signaling correlated strongly with apoptosis similarly for both age groups (Figure 3E). This positive correlation seemed paradoxical given the *in vitro* data above. However, cells did not appear to be undergoing active regulated cell death,[62] as the cellular membrane of ICOS$^+$CD38$^+$ cTfh was intact based on the exclusion of viability dye (Figure S1A), and ICOS$^+$CD38$^+$ cTfh of young and elderly adults did not demonstrate reduced mitochondrial membrane potential compared to other CD4 T cell subsets (Figure S4I). Thus, although pro-apoptotic genes may increase with age, resistance to apoptosis could be linked to the induction of pro-survival genes. The expression of anti-apoptotic genes *BCL2A1* and *MCL1* correlated with the GSVA scores for TNF-NF-κB signaling in all adults (Figures 3F and S4J). Similarly, the expression of Survivin (gene name *BIRC5*; Figures 1F and S4K), a cIAP family member that can restrain caspase-3 activation,[63] was high in ICOS$^+$CD38$^+$ cTfh. Thus, together with the reduced viability *in vitro* with TNF blockade, these data suggest that TNF-NF-κB signaling may be necessary to counterbalance pro-apoptotic effects and foster cell survival circuits.

Vaccination elicits discordant transcriptional pathway responses with aging in ICOS$^+$CD38$^+$ cTfh

To better understand the full spectrum of transcriptional changes in cTfh during aging, we analyzed the vaccine-induced transcriptional signatures in ICOS$^+$CD38$^+$ cTfh on day 7 post-vaccination compared to day 0 for young versus elderly adults. Overall, influenza vaccination was associated with relatively modest changes in transcriptional profiles in ICOS$^+$CD38$^+$ cTfh from young and elderly adults (Figure 4A), suggesting that pre-vaccination ICOS$^+$CD38$^+$ cTfh share many transcriptional characteristics with these cells post-vaccination.

We then used pathway enrichment combined with pre-ranked GSEA to compare transcriptional signatures from ICOS$^+$CD38$^+$ cTfh from young versus elderly adults. Clear enrichment patterns were observed for many key gene sets. However, overall, the enrichment patterns were only concordant between young and elderly adults for ~1/3 of the Hallmark gene sets examined (Figures 4B, and S4L; Table S2), suggesting distinct biology for this cell type in elderly versus young adults. For example, TGF-β signaling displayed reduced enrichment at day 7 compared to day 0 in ICOS$^+$CD38$^+$ cTfh from both young and elderly adults (Figure 4C). In contrast, in young adults, there was positive enrichment (associated with upregulation at day 7) for the E2F target gene set in ICOS$^+$CD38$^+$ cTfh, whereas elderly adults had negative enrichment for this pathway (Figure 4D). The opposite pattern was observed for IL-2-STAT5 (Figure 4E) and TNF-NF-κB signaling (Figure 4F), both of which were enriched in the elderly adults compared to the young adults. In general, ICOS$^+$CD38$^+$ cTfh from the young adults enriched positively for signatures of regulation of proliferation and Myc biology, but negatively for signatures of inflammatory signaling. In contrast, ICOS$^+$CD38$^+$ cTfh from the elderly adults enriched positively for metabolic pathways and inflammatory signaling. These results demonstrate multiple pathway-level differences with aging in ICOS$^+$CD38$^+$ cTfh after influenza vaccination.

Age-related differences preferentially revealed by CD4 T cell subset analysis

We next hypothesized that the age-related differences in cellular pathways may be distinct in different CD4 T cell subsets. We therefore compared enrichment for 9 Hallmark gene sets by GSEA in naive CD4 T cells, ICOS$^-$CD38$^-$ cTfh, and ICOS$^+$CD38$^+$ cTfh from young and elderly adults before (day 0) and after (day 7) influenza vaccination (Figures 5A–5I, S5A, and S5B; Table S2). These analyses revealed several key findings. First, consistent with our data in ICOS$^+$CD38$^+$ cTfh (Figure 1), most of the pathways showed only weak differences with aging at baseline. Two exceptions included a moderate enrichment of Myc targets (Figure 5D) in ICOS$^-$CD38$^-$ cTfh and ICOS$^+$CD38$^+$ cTfh from the elderly adults at baseline and an enrichment of oxidative phosphorylation (Figure 5F) in the ICOS$^-$CD38$^-$ cTfh from the young adults at day 0. Second, the overall similarity at baseline was contrasted by substantial differences following vaccination. Of all of the gene sets, 57% changed in enrichment direction (i.e., from young to elderly or vice versa) for ICOS$^+$CD38$^+$ cTfh between days 0 and 7, compared with 30% for naive CD4 between days 0 and 7. However, one of the most clear patterns was the uncovering of an underlying bias for inflammatory signatures, including TNF-NF-κB, inflammatory response, and IL-2-STAT5 gene sets to be preferentially enriched in the CD4 T cells of the elderly adults, often with the greatest enrichment in the ICOS$^+$CD38$^+$ cTfh subset (Figures 5A–5C, and 5J). Third, ICOS$^+$CD38$^+$ cTfh showed the greatest dynamic range of the 3 T cell subsets, based on the difference with aging in the day 7 and day 0 normalized enrichment scores per subset (Figure 5J). Whether these differences reflect differential systemic induction of inflammation upon vaccination, distinct abilities of T cells to induce transcriptional responses related to these pathways due to aging, or both, remain to be determined.

The different signatures of ICOS$^+$CD38$^+$ cTfh from young and elderly adults are most apparent at day 7 post-vaccination

Differences in the transcriptional profiles of CD4 T cells with aging were most prominent in ICOS$^+$CD38$^+$ cTfh at the cellular pathway level following influenza vaccination (Figure 5). We next wanted to determine whether a whole-blood baseline gene signature of aging would be reflected in the same manner and whether vaccination was necessary to identify the features of aging.

To test this idea, baseline whole-blood microarray data from the full study cohort (27 young and 35 elderly adults, Immport SDY739) was used to assess differential gene expression with aging, using the same cohort from which the adults for the RNA-seq (Figures 1, 2, 3, 4, and 5) were derived. From these data, we constructed signatures of youth (354 genes upregulated in the young) or aging (232 genes upregulated in the elderly) (Figure S6A; Table S5). These signatures were then used to test whole-blood microarray data from other years' cohorts from the

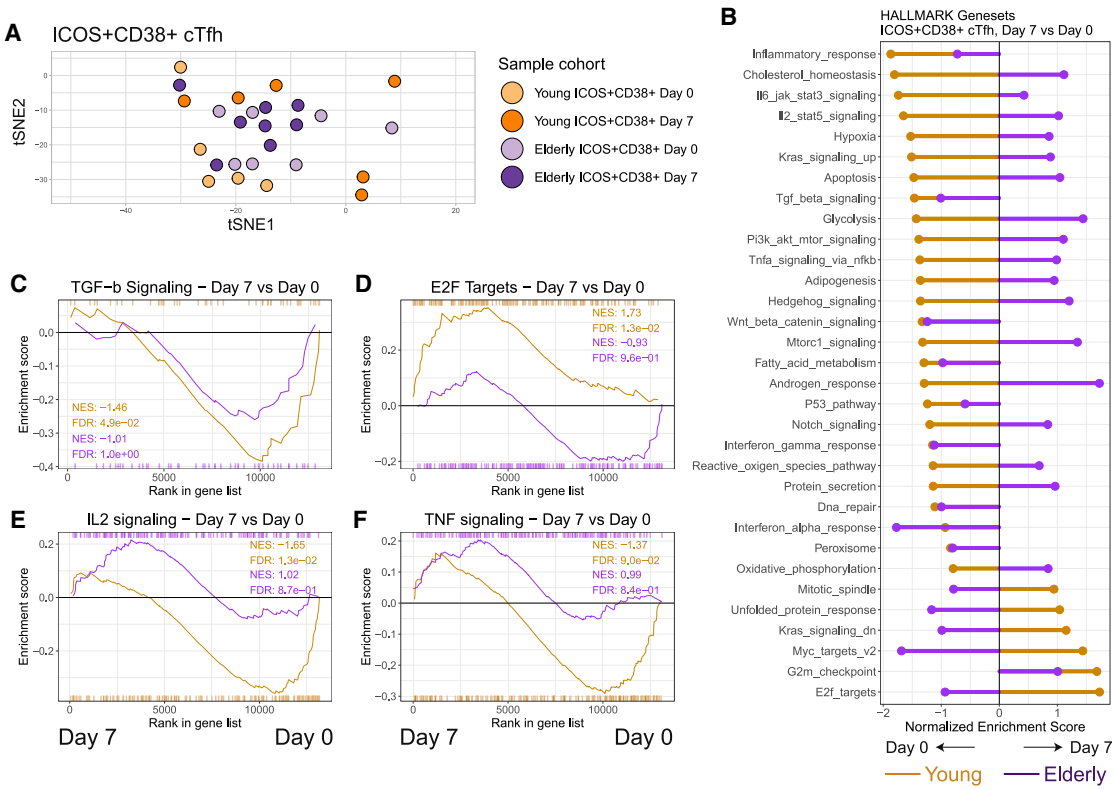

Figure 4. Age-dependent differences in transcriptional profiles of ICOS$^+$CD38$^+$ cTfh

(A) t-Distributed stochastic neighbor embedding (t-SNE) analysis was performed for all CD4 T cell subsets. ICOS$^+$CD38$^+$ cTfh shown before and after vaccination for young (n = 6) and elderly (n = 8) adults.

(B) Aggregated GSEA results for Hallmark gene sets comparing day 7 versus day 0 for ICOS$^+$CD38$^+$ cTfh in young (orange) and elderly (purple) adults.

(C–F) GSEA shown for day 7 versus day 0 for ICOS$^+$CD38$^+$ cTfh from young (orange) and elderly (purple) adults for TGF-β signaling (C), E2F targets (D), IL-2 signaling (E), and TNF-NF-κB signaling (F) gene sets.

same study.[64,65] We found strong enrichment of the signatures of youth and aging in the young and elderly adults, respectively (Figure 6A). The signature of youth had Gene Ontology terms for RNA metabolism, whereas the signature of aging had terms for fatty acid metabolism and cytoskeletal regulation (Figure S6B), in agreement with other signatures of aging.[33]

To further validate these signatures, we identified several published studies[16,66–68] that generated whole-blood transcriptional profiles on adults younger than age 40 or older than age 65 (Table S6). From these data, we performed differential expression analysis of young compared to elderly adults in multiple geographically distinct studies and again found robust enrichment for these signatures in the external datasets (Figures 6B and S6C). To test these signatures on continuous (rather than cohorted) data, GSVA scores for the signatures of youth and aging were compared against the Nanostring data for adults in a large cohort (n = 986) across lifespan (Milieu Intérieur cohort[68]). In this cohort, the signature of youth negatively correlated with age (Pearson r = −0.28, p = 8.6×10^{-20}, n = 986) and the signature of aging positively correlated with age (Pearson r = 0.31, p = 4.6×10^{-23}) (Figure S6D). These results demonstrate conserved gene expression patterns for youth and aging in whole-blood transcriptional profiling data in multiple published studies.

We next tested whether the signatures of youth and aging could be discerned in the CD4 T cell subsets examined above before and after influenza vaccination. For example, the signature of youth was positively enriched in the young cohort in all of the subsets at day 0. However, this signature of youth was most strongly enriched in the ICOS$^+$CD38$^+$ cTfh at day 7 after vaccination (Figures 6C and S6E). Similarly, the signature of aging was evident at day 0, such as in naive CD4 T cells from the elderly adults. Again, however, the strongest enrichment of the aging signature was revealed in the ICOS$^+$CD38$^+$ cTfh after vaccination (Figures 6C and S6E). These data demonstrated that ICOS$^+$CD38$^+$ cTfh are susceptible to immunologic perturbation with influenza vaccination and sensitively reflect general immunological or organismal environment of youth and aging in the cellular transcriptional program.

DISCUSSION

Induction of protective antibody responses is the goal of most vaccines. Many vaccines are less effective in elderly adults, but the underlying causes, including how aging affects Tfh and B cell responses, remain poorly understood. In this study, we examined the cTfh response to vaccination in young and elderly adults to interrogate the effects of aging on Tfh. There were several key

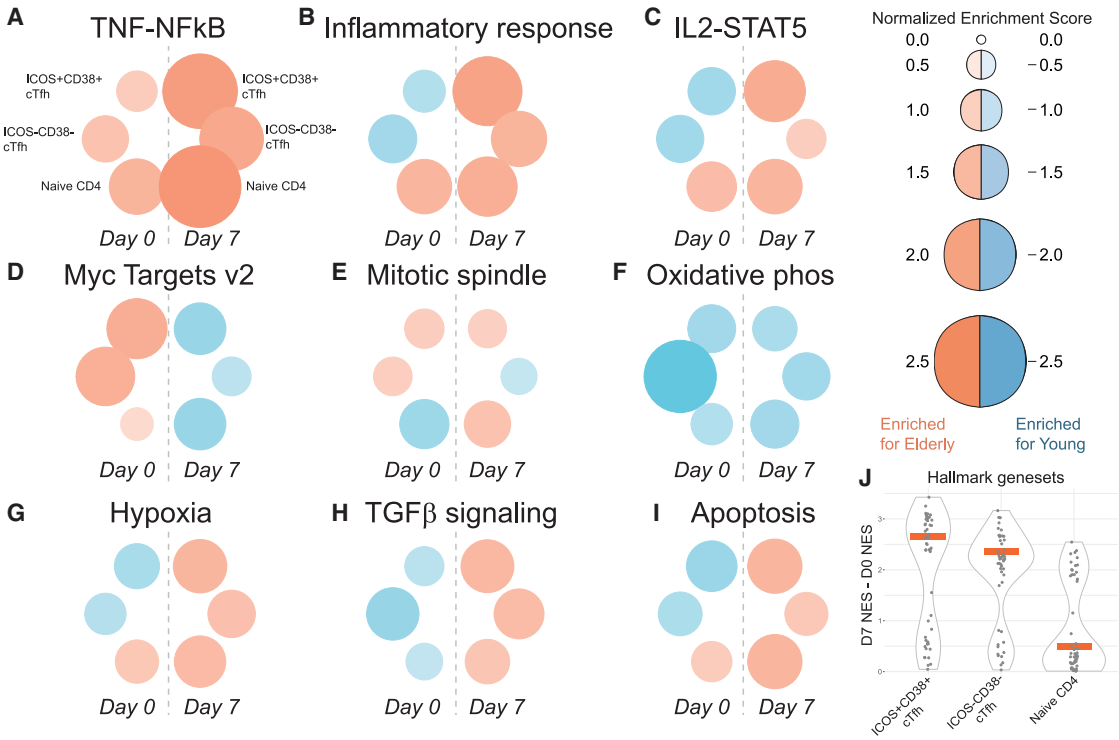

Figure 5. Age-related differences in signaling pathways are preferentially revealed by subset and time point

(A–I) GSEA performed to compare young versus elderly for each CD4 T cell subset for each time point. Normalized enrichment score shown as circle size and color.

(J) "Delta-NES" score was calculated by subtracting the day 0 NES score from the day 7 NES score with aging for each gene set for each subset. Each dot represents 1 gene set. The red bar indicates median.

observations from these studies. First, despite the similar magnitude of responses to vaccination and in the expression of individual Tfh-associated genes, ICOS$^+$CD38$^+$ cTfh from young and elderly adults differed in network level transcriptional signatures, revealing underlying changes in key biological pathways not apparent at the level of individual genes. Second, signatures of inflammatory responses, IL-2-STAT5 signaling, and TNF-NF-κB signaling in particular were substantially stronger in ICOS$^+$CD38$^+$ cTfh from elderly adults. Third, vaccine-induced ICOS$^+$CD38$^+$ cTfh reflected underlying signatures of aging versus youth more strongly than ICOS$^-$CD38$^-$ cTfh or naive CD4 T cells. These latter observations indicate that recently activated cTfh may function as biosensors of underlying inflammatory and/or host physiological environments and reflect underlying features of "immune health."

Increased baseline inflammation in elderly adults has often been associated with declines in overall health[69] and, in particular, the TNF-NF-κB pathway has been implicated in many pathological changes with aging. However, these correlations are at odds with the apparent detrimental effects of TNF pathway blockade on vaccination[23–25] that suggest that blocking residual TNF signaling impairs, rather than enhances, vaccine-induced antibody responses. Moreover, data from mice indicate a key role for TNF in GC responses.[26–29] Thus, how TNF-NF-κB signaling regulates GC-dependent, vaccine-induced immunity in elderly adults remains incompletely understood. Here, TNF-NF-κB signaling was correlated with quantitatively better antibody responses, suggesting a positive role for TNF signaling in human GC-dependent immune responses. ICOS$^+$CD38$^+$ cTfh displayed a strong transcriptional signature of TNF-NF-κB pathway signaling in all adults, especially the elderly, and blockade of TNF signaling *in vitro* led to reduced Ig production by B cells. Furthermore, these *in vitro* studies indicated reduced cellular survival upon blockade of TNF signaling. Our results point to a pro-survival effect of TNF signaling. likely due to the effects of TNF signaling on cTfh and/or TNF production by cTfh. Despite the increased expression of pro-apoptotic Bcl family members such as *BID* in ICOS$^+$CD38$^+$ cTfh, there was a concomitant increase in the expression of pro-survival factors *BCL2A1* and *MCL1* that strongly correlated with TNF-NF-κB GSVA scores in ICOS$^+$CD38$^+$ cTfh at day 7, suggesting a TNF-NF-κB-dependent survival signal in activated cTfh. These genes have NF-κB binding sites in their respective promoter sequences[70,71] linking TNF signaling to a potential pro-survival circuit in these cells. Moreover, TNFR1 expression in ICOS$^+$CD38$^+$ cTfh at day 7 positively correlated with neutralizing antibody production. These data are in agreement with and may provide an explanation for clinical data from patients receiving therapeutic TNF blockade demonstrating fewer GC reactions[72] and attenuated antibody responses to influenza vaccination.[25] Whether TNF signaling in GC-Tfh regulates proteins involved in providing B cell help such as ICOS, CD40L, and IL-21[43] will be interesting to investigate in future studies.

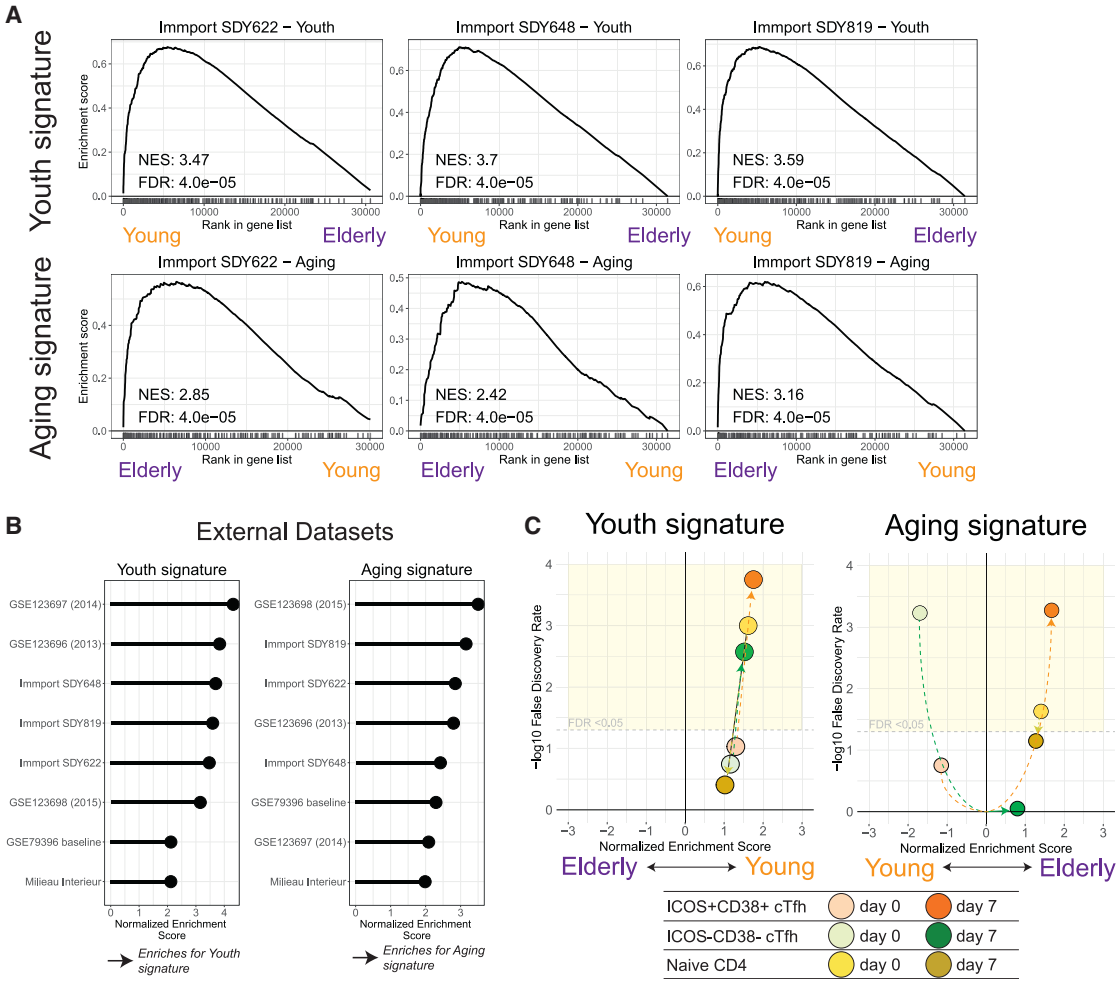

Figure 6. ICOS$^+$CD38$^+$ cTfh transcriptional profiles reveal signatures of aging

(A) Signatures for youth and aging were constructed from the differential expression of young versus elderly whole-blood transcriptional profiling from Immport study SDY739. These signatures were tested by pre-ranked GSEA for other vaccine years in this study (SDY622, SDY648, and SDY819).

(B) The signatures of youth and aging were validated against publicly available whole-blood transcriptional profiles (GSE accessions GEO: GSE123696, GEO: GSE123697, GEO: GSE123698, and GEO: GSE79396) and Nanostring target profiling (EGAS00001002460, Milieu Intérieur) for young (ages 20–40) and elderly (ages 60 and older) adults. Normalized enrichment score (NES) shown for youth (left) and aging (right) signatures.

(C) CD4 T cell subsets were tested for signatures of youth and aging. Naive (yellow), ICOS$^-$CD38$^-$ cTfh (green), and ICOS$^+$CD38$^+$ cTfh (orange) are shown, with days 0 and 7 connected by dotted lines. The yellow region indicates FDR < 0.05.

Previously, we identified correlations between cTfh responses and influenza-specific IgG antibody responses in young adults but not in elderly adults.[38] Here, we observed a similar magnitude of the total ICOS$^+$CD38$^+$ cTfh response following vaccination in young and elderly adults, and the cTfh responses correlated with the plasmablast response. Nevertheless, vaccine-induced neutralizing antibody titers were slightly lower in elderly compared to young adults. ICOS$^+$CD38$^+$ cTfh preferentially reflected underlying inflammatory and age-related biological signatures 7 days after influenza vaccination, compared to ICOS$^-$CD38$^-$ cTfh or naive CD4 T cells. There are several potential reasons for this. For example, the increase in the ICOS$^+$CD38$^+$ cTfh subset at day 7 post-vaccination likely reflects an induction and/or reactivation of influenza-specific CD4 T cells.[41] Thus, these influenza-specific T cells may be qualitatively different from the ICOS$^+$CD38$^+$ cTfh circulating at baseline. However, a second related feature of these vaccine-induced cTfh may be the synchronous nature of the responses. The ICOS$^+$CD38$^+$ cTfh responses at baseline likely reflect ongoing chronically activated cTfh or cTfh in different phases of acute activation. In contrast, the vaccine-induced cTfh are aligned in their activation and differentiation kinetics, perhaps resulting in more focused transcriptional circuitry. Recent activation may also facilitate sensitivity and/or changes in inflammatory cytokine signaling, as has been suggested for NF-κB signaling in GC B cells.[73] In addition to enrichment for TNF-NF-κB signaling and a broader signature of aging, activated cTfh also displayed transcriptional evidence of age-dependent alterations in many other inflammatory pathways, including IL-2-STAT5 signaling, TGF-β pathway signaling, and IL-6-JAK-STAT3 signaling. These observations were notable given

the regulatory role of IL-2-STAT5 signaling in Tfh differentiation.[50,74,75] The data presented here point to the use of vaccine-induced ICOS$^+$CD38$^+$ cTfh as a window into potentially broader underlying host immunological changes.

To aid in understanding the impact of aging on cTfh, we constructed transcriptional signatures of youth and aging based on whole-blood transcriptional profiling from 27 young adults and 34 elderly adults. These signatures were then validated using multiple, geographically distinct cohorts, representing a total of 566 young adult samples and 344 elderly adult samples. Furthermore, the GSVA scores for the signatures of youth and aging correlated with age as a continuous variable in the Milieu Intérieur study of nearly 1,000 adults[68], with age explaining 7.8%–9.6% of the variance in the GSVA scores of our signatures. Overall, these data indicated that the highest enrichment scores for our signatures of youth and aging were in the day 7 ICOS$^+$CD38$^+$ cTfh subset. These observations suggest that cTfh, and especially the synchronized, vaccine-induced cTfh at day 7 after influenza vaccination, may be sensitive biosensors of underlying features of immune inflammation or immune health.

Studies of vaccine-induced immune responses during aging are needed to understand poor immune responses in elderly adults, who are at heightened risk from infection. These data not only identify roles for inflammatory pathways in alterations of cTfh during aging but also point to vaccine-induced cTfh as a cell type that may provide a window into changes in overall immune health and fitness.

Limitations of study

Aging is a complex phenomenon, and as a result, the number of participants evaluated here in the RNA-seq studies may not fully reflect the subtleties or full heterogeneity of aging across individuals. Moreover, our study recruited community-dwelling, relatively healthy adults. As a result, evaluation of the effects of comorbidities and concomitant medications was not possible here. Only one type of inactivated influenza vaccine was used for participants in these studies, and it may be interesting to extend these observations to other inactivated influenza vaccines or even other types of vaccines. The extent to which a circulating subset, ICOS$^+$CD38$^+$ cTfh, can serve as a cellular biomarker will need to be further assessed in conjunction with studies of age-associated changes in lymphoid Tfh through access to lymph node material or perhaps lymph. Finally, future studies will be needed to fully understand how aging and TNF signaling affect Tfh, and by extension, vaccine responses.

STAR★METHODS

Detailed methods are provided in the online version of this paper and include the following:

SUPPLEMENTAL INFORMATION

Supplemental information can be found online at https://doi.org/10.1016/j.xcrm.2021.100262.

ACKNOWLEDGMENTS

We would like to thank the study participants, as well as the members of the Wherry lab who provided critical feedback. We thank the Next Generation Sequencing Core, the Flow Cytometry Core, and the Human Immunology Core at the University of Pennsylvania for their assistance in these studies. This work was supported by NIH grants AI114852 and AG047773 (to R.S.H.), the Pediatric Infectious Diseases Society Fellowship Award, the National Center for Advancing Translational Sciences of the National Institutes of Health under award no. KL2TR001879 (to L.A.V.), and a Mentored Research Scholar Award from the Penn Center for AIDS Research (CFAR) (to L.A.V.), an NIH-funded program (P30 AI 045008), as well as R50 CA211199 (to A.V.K.). K.E.S. was supported in part by the NIH/National Institute on Aging Claude D. Pepper Older Americans Independence Centers (grant no. AG028716). D.H.C. was supported by Veterans Affairs and AI108972. This work was additionally supported by NIH grants AI105343, AI112521, AI082630, AI201085, and AI117950 (to E.J.W.), as well as US Broad Agency Announcement HHSN272201100018C (to K.E.S., H.C.J.E., and E.J.W.) and the Allen Institute for Immunology funding to E.J.W. E.J.W. is also supported by the Parker Institute for Cancer Immunotherapy which supports the cancer immunology program at the University of Pennsylvania.

AUTHOR CONTRIBUTIONS

R.S.H., L.V.S., L.A.V., A.M., B.B., S.M., and D.H.C. designed and performed the experiments. R.S.H. and E.J.W. conceived the overall design. S.K., R.K.K., and H.C.J.E. performed and analyzed the antibody assays. A.V.K. analyzed Immport studies SDY622, SDY648, SDY739, and SDY819. C.A. assisted with Milieu Intérieur. S.A.D. and K.E.S. conducted the vaccine study. R.S.H. and E.J.W. wrote the manuscript. All of the authors analyzed the data, discussed the results, and commented on the manuscript.

DECLARATION OF INTERESTS

The authors declare no competing interests. E.J.W. consults or is an advisor for Merck, Elstar, Janssen, Related Sciences, Synthekine, and Surface Oncology, unrelated to the present study. E.J.W. is a founder of Surface Oncology and Arsenal Biosciences, unrelated to the present study. E.J.W. is an inventor on a patent (US patent no. 10,370,446) submitted by Emory University that covers the use of PD-1 blockade to treat infections and cancer.

Received: December 23, 2019
Revised: December 31, 2020
Accepted: April 6, 2021
Published: May 7, 2021

REFERENCES

1. Lang, P.-O., Mendes, A., Socquet, J., Assir, N., Govind, S., and Aspinall, R. (2012). Effectiveness of influenza vaccine in aging and older adults: comprehensive analysis of the evidence. Clin. Interv. Aging *7*, 55–64.
2. Goronzy, J.J., and Weyand, C.M. (2013). Understanding immunosenescence to improve responses to vaccines. Nat. Immunol. *14*, 428–436.
3. Gustafson, C.E., Weyand, C.M., and Goronzy, J.J. (2018). T follicular helper cell development and functionality in immune ageing. Clin. Sci. (Lond.) *132*, 1925–1935.
4. Henry, C., Zheng, N.-Y., Huang, M., Cabanov, A., Rojas, K.T., Kaur, K., Andrews, S.F., Palm, A.E., Chen, Y.-Q., Li, Y., et al. (2019). Influenza Virus Vaccination Elicits Poorly Adapted B Cell Responses in Elderly Individuals. Cell Host Microbe *25*, 357–366.e6.
5. Xu, W., and Larbi, A. (2017). Markers of T Cell Senescence in Humans. Int. J. Mol. Sci. *18*, E1742.
6. Fülöp, T., Dupuis, G., Witkowski, J.M., and Larbi, A. (2016). The Role of Immunosenescence in the Development of Age-Related Diseases. Rev. Invest. Clin. *68*, 84–91.
7. Fulop, T., Larbi, A., Dupuis, G., Le Page, A., Frost, E.H., Cohen, A.A., Witkowski, J.M., and Franceschi, C. (2018). Immunosenescence and Inflamm-Aging As Two Sides of the Same Coin: Friends or Foes? Front. Immunol. *8*, 1960.
8. Goronzy, J.J., Li, G., Yu, M., and Weyand, C.M. (2012). Signaling pathways in aged T cells - a reflection of T cell differentiation, cell senescence and host environment. Semin. Immunol. *24*, 365–372.
9. Frasca, D., Diaz, A., Romero, M., Landin, A.M., Phillips, M., Lechner, S.C., Ryan, J.G., and Blomberg, B.B. (2010). Intrinsic defects in B cell response to seasonal influenza vaccination in elderly humans. Vaccine *28*, 8077–8084.
10. Larbi, A., Pawelec, G., Wong, S.C., Goldeck, D., Tai, J.J.-Y., and Fulop, T. (2011). Impact of age on T cell signaling: a general defect or specific alterations? Ageing Res. Rev. *10*, 370–378.
11. Fulop, T., Witkowski, J.M., Le Page, A., Fortin, C., Pawelec, G., and Larbi, A. (2017). Intracellular signalling pathways: targets to reverse immunosenescence. Clin. Exp. Immunol. *187*, 35–43.
12. Frasca, D., Diaz, A., Romero, M., Landin, A.M., and Blomberg, B.B. (2014). High TNF-α levels in resting B cells negatively correlate with their response. Exp. Gerontol. *54*, 116–122.
13. Sage, P.T., Tan, C.L., Freeman, G.J., Haigis, M., and Sharpe, A.H. (2015). Defective TFH Cell Function and Increased TFR Cells Contribute to Defective Antibody Production in Aging. Cell Rep. *12*, 163–171.
14. Lambert, N.D., Ovsyannikova, I.G., Pankratz, V.S., Jacobson, R.M., and Poland, G.A. (2012). Understanding the immune response to seasonal influenza vaccination in older adults: a systems biology approach. Expert Rev. Vaccines *11*, 985–994.
15. Ciabattini, A., Nardini, C., Santoro, F., Garagnani, P., Franceschi, C., and Medaglini, D. (2018). Vaccination in the elderly: the challenge of immune changes with aging. Semin. Immunol. *40*, 83–94.
16. Li, S., Sullivan, N.L., Rouphael, N., Yu, T., Banton, S., Maddur, M.S., McCausland, M., Chiu, C., Canniff, J., Dubey, S., et al. (2017). Metabolic Phenotypes of Response to Vaccination in Humans. Cell *169*, 862–877.e17.
17. Nakaya, H.I., Hagan, T., Duraisingham, S.S., Lee, E.K., Kwissa, M., Rouphael, N., Frasca, D., Gersten, M., Mehta, A.K., Gaujoux, R., et al. (2015). Systems Analysis of Immunity to Influenza Vaccination across Multiple Years and in Diverse Populations Reveals Shared Molecular Signatures. Immunity *43*, 1186–1198.
18. Crotty, S. (2011). Follicular helper CD4 T cells (TFH). Annu. Rev. Immunol. *29*, 621–663.
19. Zhang, Q., Lenardo, M.J., and Baltimore, D. (2017). 30 Years of NF-κB: A Blossoming of Relevance to Human Pathobiology. Cell *168*, 37–57.
20. Ferrucci, L., Corsi, A., Lauretani, F., Bandinelli, S., Bartali, B., Taub, D.D., Guralnik, J.M., and Longo, D.L. (2005). The origins of age-related proinflammatory state. Blood *105*, 2294–2299.
21. Shive, C.L., Judge, C.J., Clagett, B., Kalayjian, R.C., Osborn, M., Sherman, K.E., Fichtenbaum, C., Gandhi, R.T., Kang, M., Popkin, D.L., et al. (2018). Pre-vaccine plasma levels of soluble inflammatory indices negatively predict responses to HAV, HBV, and tetanus vaccines in HCV and HIV infection. Vaccine *36*, 453–460.
22. Tebas, P., Frank, I., Lewis, M., Quinn, J., Zifchak, L., Thomas, A., Kenney, T., Kappes, R., Wagner, W., Maffei, K., and Sullivan, K.; Center for AIDS Research and Clinical Trials Unit of the University of Pennsylvania (2010). Poor immunogenicity of the H1N1 2009 vaccine in well controlled HIV-infected individuals. AIDS *24*, 2187–2192.
23. Salinas, G.F., De Rycke, L., Barendregt, B., Paramarta, J.E., Hreggvidsdottir, H., Cantaert, T., van der Burg, M., Tak, P.P., and Baeten, D. (2013). Anti-TNF treatment blocks the induction of T cell-dependent humoral responses. Ann. Rheum. Dis. *72*, 1037–1043.
24. Elkayam, O., Caspi, D., Reitblatt, T., Charboneau, D., and Rubins, J.B. (2004). The effect of tumor necrosis factor blockade on the response to pneumococcal vaccination in patients with rheumatoid arthritis and ankylosing spondylitis. Semin. Arthritis Rheum. *33*, 283–288.
25. Kobie, J.J., Zheng, B., Bryk, P., Barnes, M., Ritchlin, C.T., Tabechian, D.A., Anandarajah, A.P., Looney, R.J., Thiele, R.G., Anolik, J.H., et al. (2011). Decreased influenza-specific B cell responses in rheumatoid arthritis patients treated with anti-tumor necrosis factor. Arthritis Res. Ther. *13*, R209.
26. Matsumoto, M., Mariathasan, S., Nahm, M.H., Baranyay, F., Peschon, J.J., and Chaplin, D.D. (1996). Role of lymphotoxin and the type I TNF receptor in the formation of germinal centers. Science *271*, 1289–1291.
27. Le Hir, M., Bluethmann, H., Kosco-Vilbois, M.H., Müller, M., di Padova, F., Moore, M., Ryffel, B., and Eugster, H.P. (1996). Differentiation of follicular dendritic cells and full antibody responses require tumor necrosis factor receptor-1 signaling. J. Exp. Med. *183*, 2367–2372.
28. Pasparakis, M., Alexopoulou, L., Episkopou, V., and Kollias, G. (1996). Immune and inflammatory responses in TNF alpha-deficient mice: a critical requirement for TNF alpha in the formation of primary B cell follicles, follicular dendritic cell networks and germinal centers, and in the maturation of the humoral immune response. J. Exp. Med. *184*, 1397–1411.
29. Marino, M.W., Dunn, A., Grail, D., Inglese, M., Noguchi, Y., Richards, E., Jungbluth, A., Wada, H., Moore, M., Williamson, B., et al. (1997). Characterization of tumor necrosis factor-deficient mice. Proc. Natl. Acad. Sci. USA *94*, 8093–8098.
30. Hu, R., Kagele, D.A., Huffaker, T.B., Runtsch, M.C., Alexander, M., Liu, J., Bake, E., Su, W., Williams, M.A., Rao, D.S., et al. (2014). miR-155 promotes T follicular helper cell accumulation during chronic, low-grade inflammation. Immunity *41*, 605–619.
31. Thai, T.H., Calado, D.P., Casola, S., Ansel, K.M., Xiao, C., Xue, Y., Murphy, A., Frendewey, D., Valenzuela, D., Kutok, J.L., et al. (2007). Regulation of the germinal center response by microRNA-155. Science *316*, 604–608.
32. Liu, W.-H., Kang, S.G., Huang, Z., Wu, C.-J., Jin, H.Y., Maine, C.J., Liu, Y., Shepherd, J., Sabouri-Ghomi, M., Gonzalez-Martin, A., et al. (2016). A miR-155–Peli1–c-Rel pathway controls the generation and function of T follicular helper cells. J. Exp. Med. *213*, 1901–1919.
33. Peters, M.J., Joehanes, R., Pilling, L.C., Schurmann, C., Conneely, K.N., Powell, J., Reinmaa, E., Sutphin, G.L., Zhernakova, A., Schramm, K., et al.; NABEC/UKBEC Consortium (2015). The transcriptional landscape of age in human peripheral blood. Nat. Commun. *6*, 8570.
34. Lefebvre, J.S., Masters, A.R., Hopkins, J.W., and Haynes, L. (2016). Age-related impairment of humoral response to influenza is associated with changes in antigen specific T follicular helper cell responses. Sci. Rep. *6*, 25051.
35. Morita, R., Schmitt, N., Bentebibel, S.E., Ranganathan, R., Bourdery, L., Zurawski, G., Foucat, E., Dullaers, M., Oh, S., Sabzghabaei, N., et al. (2011). Human blood CXCR5(+)CD4(+) T cells are counterparts of T

follicular cells and contain specific subsets that differentially support antibody secretion. Immunity *34*, 108–121.

36. Locci, M., Havenar-Daughton, C., Landais, E., Wu, J., Kroenke, M.A., Arlehamn, C.L., Su, L.F., Cubas, R., Davis, M.M., Sette, A., et al.; International AIDS Vaccine Initiative Protocol C Principal Investigators (2013). Human circulating PD-1+CXCR3-CXCR5+ memory Tfh cells are highly functional and correlate with broadly neutralizing HIV antibody responses. Immunity *39*, 758–769.

37. Obeng-Adjei, N., Portugal, S., Tran, T.M., Yazew, T.B., Skinner, J., Li, S., Jain, A., Felgner, P.L., Doumbo, O.K., Kayentao, K., et al. (2015). Circulating Th1-Cell-type Tfh Cells that Exhibit Impaired B Cell Help Are Preferentially Activated during Acute Malaria in Children. Cell Rep. *13*, 425–439.

38. Herati, R.S., Reuter, M.A., Dolfi, D.V., Mansfield, K.D., Aung, H., Badwan, O.Z., Kurupati, R.K., Kannan, S., Ertl, H., Schmader, K.E., et al. (2014). Circulating CXCR5+PD-1+ response predicts influenza vaccine antibody responses in young adults but not elderly adults. J. Immunol. *193*, 3528–3537.

39. Bentebibel, S.E., Lopez, S., Obermoser, G., Schmitt, N., Mueller, C., Harrod, C., Flano, E., Mejias, A., Albrecht, R.A., Blankenship, D., et al. (2013). Induction of ICOS+CXCR3+CXCR5+ TH cells correlates with antibody responses to influenza vaccination. Sci. Transl. Med. *5*, 176ra32.

40. Bentebibel, S.E., Khurana, S., Schmitt, N., Kurup, P., Mueller, C., Obermoser, G., Palucka, A.K., Albrecht, R.A., Garcia-Sastre, A., Golding, H., and Ueno, H. (2016). ICOS(+)PD-1(+)CXCR3(+) T follicular helper cells contribute to the generation of high-avidity antibodies following influenza vaccination. Sci. Rep. *6*, 26494.

41. Herati, R.S., Muselman, A., Vella, L., Bengsch, B., Parkhouse, K., Del Alcazar, D., Kotzin, J., Doyle, S.A., Tebas, P., Hensley, S.E., et al. (2017). Successive annual influenza vaccination induces a recurrent oligoclonotypic memory response in circulating T follicular helper cells. Sci. Immunol. *2*, eaag2152.

42. Vella, L.A., Buggert, M., Manne, S., Herati, R.S., Sayin, I., Kuri-Cervantes, L., Bukh Brody, I., O'Boyle, K.C., Kaprielian, H., Giles, J.R., et al. (2019). T follicular helper cells in human efferent lymph retain lymphoid characteristics. J. Clin. Invest. *129*, 3185–3200.

43. Crotty, S. (2014). T follicular helper cell differentiation, function, and roles in disease. Immunity *41*, 529–542.

44. Xu, W., Zhao, X., Wang, X., Feng, H., Gou, M., Jin, W., Wang, X., Liu, X., and Dong, C. (2019). The Transcription Factor Tox2 Drives T Follicular Helper Cell Development via Regulating Chromatin Accessibility. Immunity *51*, 826–839.e5.

45. Vinuesa, C.G., Linterman, M.A., Yu, D., and MacLennan, I.C.M. (2016). Follicular Helper T Cells. Annu. Rev. Immunol. *34*, 335–368.

46. Crotty, S. (2019). T Follicular Helper Cell Biology: A Decade of Discovery and Diseases. Immunity *50*, 1132–1148.

47. Subramanian, A., Tamayo, P., Mootha, V.K., Mukherjee, S., Ebert, B.L., Gillette, M.A., Paulovich, A., Pomeroy, S.L., Golub, T.R., Lander, E.S., and Mesirov, J.P. (2005). Gene set enrichment analysis: a knowledge-based approach for interpreting genome-wide expression profiles. Proc. Natl. Acad. Sci. USA *102*, 15545–15550.

48. Johnston, R.J., Poholek, A.C., DiToro, D., Yusuf, I., Eto, D., Barnett, B., Dent, A.L., Craft, J., and Crotty, S. (2009). Bcl6 and Blimp-1 are reciprocal and antagonistic regulators of T follicular helper cell differentiation. Science *325*, 1006–1010.

49. Marshall, H.D., Chandele, A., Jung, Y.W., Meng, H., Poholek, A.C., Parish, I.A., Rutishauser, R., Cui, W., Kleinstein, S.H., Craft, J., and Kaech, S.M. (2011). Differential expression of Ly6C and T-bet distinguish effector and memory Th1 CD4(+) cell properties during viral infection. Immunity *35*, 633–646.

50. Johnston, R.J., Choi, Y.S., Diamond, J.A., Yang, J.A., and Crotty, S. (2012). STAT5 is a potent negative regulator of TFH cell differentiation. J. Exp. Med. *209*, 243–250.

51. Langfelder, P., and Horvath, S. (2008). WGCNA: an R package for weighted correlation network analysis. BMC Bioinformatics *9*, 559.

52. Lambert, S.A., Jolma, A., Campitelli, L.F., Das, P.K., Yin, Y., Albu, M., Chen, X., Taipale, J., Hughes, T.R., and Weirauch, M.T. (2018). The Human Transcription Factors. Cell *172*, 650–665.

53. Krämer, A., Green, J., Pollard, J., Jr., and Tugendreich, S. (2014). Causal analysis approaches in Ingenuity Pathway Analysis. Bioinformatics *30*, 523–530.

54. Ingenuity Systems (2014). Ingenuity Upstream Regulator Analysis in IPA®. http://pages.ingenuity.com/rs/ingenuity/images/0812%20upstream_regulator_analysis_whitepaper.pdf.

55. Yang, Y., Wu, J., and Wang, J. (2016). A database and functional annotation of NF-κB target genes. Int. J. Clin. Exp. Med. *9*, 7986–7995.

56. Bruunsgaard, H., Andersen-Ranberg, K., Jeune, B., Pedersen, A.N., Skinhøj, P., and Pedersen, B.K. (1999). A high plasma concentration of TNF-alpha is associated with dementia in centenarians. J. Gerontol. A Biol. Sci. Med. Sci. *54*, M357–M364.

57. Frasca, D., and Blomberg, B.B. (2016). Inflammaging decreases adaptive and innate immune responses in mice and humans. Biogerontology *17*, 7–19.

58. Hänzelmann, S., Castelo, R., and Guinney, J. (2013). GSVA: gene set variation analysis for microarray and RNA-seq data. BMC Bioinformatics *14*, 7.

59. Mehta, A.K., Gracias, D.T., and Croft, M. (2018). TNF activity and T cells. Cytokine *101*, 14–18.

60. Haney, D., Quigley, M.F., Asher, T.E., Ambrozak, D.R., Gostick, E., Price, D.A., Douek, D.C., and Betts, M.R. (2011). Isolation of viable antigen-specific CD8+ T cells based on membrane-bound tumor necrosis factor (TNF)-α expression. J. Immunol. Methods *369*, 33–41.

61. Frasca, D., and Blomberg, B.B. (2011). Aging affects human B cell responses. J. Clin. Immunol. *31*, 430–435.

62. Galluzzi, L., and Vitale, I. (2018). Molecular mechanisms of cell death : recommendations of the Nomenclature Committee on Cell Death 2018. Cell Death Differentiation *25*, 486–541.

63. Andersson, K.M.E., Brisslert, M., Cavallini, N.F., Svensson, M.N.D., Welin, A., Erlandsson, M.C., Ciesielski, M.J., Katona, G., and Bokarewa, M.I. (2015). Survivin co-ordinates formation of follicular T-cells acting in synergy with Bcl-6. Oncotarget *6*, 20043–20057.

64. Agarwal, D., Schmader, K.E., Kossenkov, A.V., Doyle, S., Kurupati, R., and Ertl, H.C.J. (2018). Immune response to influenza vaccination in the elderly is altered by chronic medication use. Immun. Ageing *15*, 19.

65. Kurupati, R., Kossenkov, A., Haut, L., Kannan, S., Xiang, Z., Li, Y., Doyle, S., Liu, Q., Schmader, K., Showe, L., and Ertl, H. (2016). Race-related differences in antibody responses to the inactivated influenza vaccine are linked to distinct pre-vaccination gene expression profiles in blood. Oncotarget *7*, 62898–62911.

66. Alpert, A., Pickman, Y., Leipold, M., Rosenberg-Hasson, Y., Ji, X., Gaujoux, R., Rabani, H., Starosvetsky, E., Kveler, K., Schaffert, S., et al. (2019). A clinically meaningful metric of immune age derived from high-dimensional longitudinal monitoring. Nat. Med. *25*, 487–495.

67. Piasecka, B., Duffy, D., Urrutia, A., Quach, H., Patin, E., Posseme, C., Bergstedt, J., Charbit, B., Rouilly, V., MacPherson, C.R., et al.; Milieu Intérieur Consortium (2018). Distinctive roles of age, sex, and genetics in shaping transcriptional variation of human immune responses to microbial challenges. Proc. Natl. Acad. Sci. USA *115*, E488–E497.

68. Thomas, S., Rouilly, V., Patin, E., Alanio, C., Dubois, A., Delval, C., Marquier, L.-G., Fauchoux, N., Sayegrih, S., Vray, M., et al.; Milieu Intérieur Consortium (2015). The Milieu Intérieur study - an integrative approach for study of human immunological variance. Clin. Immunol. *157*, 277–293.

69. Bektas, A., Schurman, S.H., Sen, R., and Ferrucci, L. (2017). Human T cell immunosenescence and inflammation in aging. J. Leukoc. Biol. *102*, 977–988.

70. Wang, C.Y., Guttridge, D.C., Mayo, M.W., and Baldwin, A.S., Jr. (1999). NF-kappaB Induces Expression of the Bcl-2 Homologue A1/Bfl-1 To Preferentially Suppress Chemotherapy-Induced Apoptosis. Mol. Cell Biol. *19*, 5923–5929.

71. Liu, H., Yang, J., Yuan, Y., Xia, Z., Chen, M., Xie, L., Ma, X., and Wang, J. (2014). Regulation of Mcl-1 by constitutive activation of NF-kappaB contributes to cell viability in human esophageal squamous cell carcinoma cells. BMC Cancer *14*, 98.

72. Anolik, J.H., Ravikumar, R., Barnard, J., Owen, T., Almudevar, A., Milner, E.C.B., Miller, C.H., Dutcher, P.O., Hadley, J.A., and Sanz, I. (2008). Cutting edge: anti-tumor necrosis factor therapy in rheumatoid arthritis inhibits memory B lymphocytes via effects on lymphoid germinal centers and follicular dendritic cell networks. J. Immunol. *180*, 688–692.

73. Luo, W., Weisel, F., and Shlomchik, M.J. (2018). B Cell Receptor and CD40 Signaling Are Rewired for Synergistic Induction of the c-Myc Transcription Factor in Germinal Center B Cells. Immunity *48*, 313–326.e5.

74. Ray, J.P., Staron, M.M., Shyer, J.A., Ho, P.C., Marshall, H.D., Gray, S.M., Laidlaw, B.J., Araki, K., Ahmed, R., Kaech, S.M., and Craft, J. (2015). The Interleukin-2-mTORc1 Kinase Axis Defines the Signaling, Differentiation, and Metabolism of T Helper 1 and Follicular B Helper T Cells. Immunity *43*, 690–702.

75. Papillion, A., Powell, M.D., Chisolm, D.A., Bachus, H., Fuller, M.J., Weinmann, A.S., Villarino, A., O'Shea, J.J., León, B., Oestreich, K.J., and Ballesteros-Tato, A. (2019). Inhibition of IL-2 responsiveness by IL-6 is required for the generation of GC-T_{FH} cells. Sci. Immunol. *4*, eaaw7636.

76. Bolger, A.M., Lohse, M., and Usadel, B. (2014). Trimmomatic: a flexible trimmer for Illumina sequence data. Bioinformatics *30*, 2114–2120.

77. Dobin, A., Davis, C.A., Schlesinger, F., Drenkow, J., Zaleski, C., Jha, S., Batut, P., Chaisson, M., and Gingeras, T.R. (2013). STAR: ultrafast universal RNA-seq aligner. Bioinformatics *29*, 15–21.

78. Love, M.I., Huber, W., and Anders, S. (2014). Moderated estimation of fold change and dispersion for RNA-seq data with DESeq2. Genome Biol. *15*, 550.

79. Ritchie, M.E., Phipson, B., Wu, D., Hu, Y., Law, C.W., Shi, W., and Smyth, G.K. (2015). limma powers differential expression analyses for RNA-sequencing and microarray studies. Nucleic Acids Res. *43*, e47.

80. Shannon, P., Markiel, A., Ozier, O., Baliga, N.S., Wang, J.T., Ramage, D., Amin, N., Schwikowski, B., and Ideker, T. (2003). Cytoscape: a software environment for integrated models of biomolecular interaction networks. Genome Res. *13*, 2498–2504.

81. Bindea, G., Mlecnik, B., Hackl, H., Charoentong, P., Tosolini, M., Kirilovsky, A., Fridman, W.-H., Pagès, F., Trajanoski, Z., and Galon, J. (2009). ClueGO: a Cytoscape plug-in to decipher functionally grouped gene ontology and pathway annotation networks. Bioinformatics *25*, 1091–1093.

82. Tripathi, S., Pohl, M.O., Zhou, Y., Rodriguez-Frandsen, A., Wang, G., Stein, D.A., Moulton, H.M., DeJesus, P., Che, J., Mulder, L.C.F., et al. (2015). Meta- and Orthogonal Integration of Influenza "OMICs" Data Defines a Role for UBR4 in Virus Budding. Cell Host Microbe *18*, 723–735.

83. Warde-Farley, D., Donaldson, S.L., Comes, O., Zuberi, K., Badrawi, R., Chao, P., Franz, M., Grouios, C., Kazi, F., Lopes, C.T., et al. (2010). The GeneMANIA prediction server: biological network integration for gene prioritization and predicting gene function. Nucleic Acids Res. *38* (*Web Server issue*), W214–W220.

STAR★METHODS

KEY RESOURCES TABLE

REAGENT or RESOURCE	SOURCE	IDENTIFIER
Antibodies		
Anti-human CD3 (OKT3)	Biolegend	Cat # 317301; RRID:AB_571926
Anti-human CD4 (S3.5)	Thermo-Fisher	Cat # MHCD0418; RRID:AB_10376013
Anti-human CD8 (RPA-T8)	Biolegend	Cat # 301002; RRID:AB_314120
Anti-human CD14 (M5E2)	Biolegend	Cat # 301819; RRID:AB_493694
Anti-human CD16 (3G8)	Biolegend	Cat # 302017; RRID:AB_314217
Anti-human CD19 (HIB19)	Biolegend	Cat # 302217; RRID:AB_314247
Anti-human CXCR5 (RF8B2)	BD Biosciences	Cat # 563105; RRID:AB_2738008
Anti-human PD-1 (EH12.2)	BD Biosciences	Cat # 562516; RRID:AB_11153482
Anti-human ICOS (C398.4a)	Novus	Cat # NBP1-43065; RRID:AB_10006379
Anti-human CD38 (HIT2)	BD Biosciences	Cat # 563964; RRID:AB_2738515
Anti-human CD27 (O323)	Biolegend	Cat # 356429; RRID:AB_2650750
Anti-human CD45RA (HI100)	Biolegend	Cat # 304133; RRID:AB_11126164
Anti-human NFkB p50 (4D1)	Biolegend	Cat # 616701; RRID:AB_315855
Anti-human Survivin (REA459)	Miltenyi	Cat # 130-106-741; RRID:AB_2653606
Anti-human TNF (Mab11)	BD Biosciences	Cat # 554511; RRID:AB_395442
Anti-human IgM (DA4-4)	Fisher	Cat # NBP234252A; RRID:AB_2890064
Anti-human TNFR1 (W15099A)	Biolegend	Cat # 369908; RRID:AB_2650932
Chemicals, peptides, and recombinant proteins		
Ficoll-Paque PLUS	GE Healthcare	Cat # 17-1440-03
Foxp3 Transcription Factor Staining Buffer Kit	Fisher	Cat # A25866A
DiOC6(3) (3,3′-Dihexyloxacarbocyanine Iodide)	Fisher	Cat # D273; CAS 53213-82-4
Staphyloccocal Enterotoxin B	Toxin Technology	Cat # BT202; CAS 11100-45-1
Recombinant human TNF	Biolegend	Cat # 570102
Anti-human TruStain Fc-X	Biolegend	Cat # 422301; RRID:AB_2818986
MegaCD40L	Enzo	Cat # ALX-522-110-C010
TAPI-0 inhibitor	Enzo	Cat # BML-PI133-0001
Qdot 565 ITK Amino (PEG) Quantum Dots	Fisher	Cat # Q21531MP
Qdot 585 ITK Amino (PEG) Quantum Dots	Fisher	Cat # Q21511MP
BD Horizon BB515 Streptavidin	BD Biosciences	Cat # 564453; RRID:AB_2869580
Critical commercial assays		
MILLIPLEX MAP Human Cytokine/ Chemokine Magnetic Bead Panel	Millipore	Cat # HCYTOMAG-60K
Legendplex Human Immunoglobulin Isotyping Panel	Biolegend	Cat # 740639
SMARTer Ultra-Low Input RNA kit v3	Clontech	Cat # 634850
Nextera XT Library Preparation kit	Illumina	Cat # FC-131-1096
Deposited data		
RNaseq for CD4 subsets from young and elderly adults before and after influenza vaccination	This paper	GEO: GSE134416
Alpert A et al., Longitudinal tracking of whole blood gene-expression in healthy young and old individuals	Gene Expression Omnibus	GEO: GSE123696

(*Continued on next page*)

Continued

REAGENT or RESOURCE	SOURCE	IDENTIFIER
Alpert A et al., Longitudinal tracking of whole blood gene-expression in healthy young and old individuals	Gene Expression Omnibus	GEO: GSE123697
Alpert A et al., Longitudinal tracking of whole blood gene-expression in healthy young and old individuals	Gene Expression Omnibus	GEO: GSE123698
Humoral responses to Influenza vaccination in aged populations	Immport	SDY622
Humoral responses to Influenza vaccination in aged populations	Immport	SDY648
Humoral responses to Influenza vaccination in aged populations	Immport	SDY739
Humoral responses to Influenza vaccination in aged populations	Immport	SDY819
Milieu Interieur Consortium study	European Genome-phenome Archive	EGAS00001002460
Software and algorithms		
Trimmomatic	Ref[76]	Version 0.32
STAR	Ref[77]	Version 2.5.2a
PORT normalization	N/A	Version 0.85; http://bioinf.itmat.upenn.edu/benchmarking/rnaseq/port/index.php
R environment	R Foundation	Version 4.0.0
DESeq2 library	Ref[78]	Version 1.20.0
Limma library	Ref[79]	Version 3.44.3
WGCNA library	Ref[51]	Version 1.63; https://horvath.genetics.ucla.edu/html/CoexpressionNetwork/Rpackages/WGCNA/
Cytoscape	Ref[80]	https://cytoscape.org/
Custom bioinformatics scripts	N/A	https://github.com/teamTfh/cTfh_AgingSignature
Statistical analysis		
Prism 6	Graphpad software	N/A
R environment	R Foundation	version 4.0.0

RESOURCE AVAILABILITY

Lead contact

Further information and requests for resources should be directed to and will be fulfilled by the lead contact, Ramin Sedaghat Herati (ramin.herati@nyulangone.org).

Materials availability

This study did not generate new unique reagents.

Data and code availability

Transcriptional profiling data reported here are available at the Gene Expression Omnibus (GEO) under accession number GEO: GSE134416. R scripts used in analyses and figure generation are available on Github (https://github.com/teamTfh/cTfh_AgingSignature).

EXPERIMENTAL MODEL AND SUBJECT DETAILS

Flu vaccine cohorts

In the Fall of 2014, study participants were recruited and consented at the Clinical Research Unit at Duke University Medical Center (Durham, NC, USA), in accordance with the Institutional Review Boards of both Duke University (Protocol Pro00031791) and the

University of Pennsylvania (Philadelphia, PA, USA) (Protocol #812170). Adults were classified as young (30-40 years of age) or elderly (65 years of age or older) (Table S1). Adults were eligible if they were community-dwelling and had not received influenza vaccine in the prior 6 months; they were excluded if they had contraindications to influenza vaccine, active substance abuse, HIV/AIDS, clinically active malignancy, immunomodulatory medication need (i.e., chemotherapy, corticosteroids), or active illness (i.e., active respiratory tract infections). Seasonal trivalent influenza vaccine (Fluarix, GlaxoSmithKline) was administered and peripheral venous blood was drawn on days 0, 7, and 28 after vaccination. Blood was collected into heparinized tubes and shipped overnight to Philadelphia, PA. All studies were conducted according to the Declaration of Helsinki principles.

Primary cells

Primary human PBMC were obtained at the University of Pennsylvania from de-identified donors through the Human Immunology Core (see Acknowledgments) and through a separate protocol (Protocol #820151). Samples used in Figure S3E were from adults who provided informed consent in accordance with the Institutional Review Boards of the Louis Stokes Veterans Affairs Medical Center and Case Western Reserve University, as previously reported.[38] All studies were conducted according to the Declaration of Helsinki principles.

METHOD DETAILS

Flow cytometry

PBMC and plasma were isolated using Ficoll-Paque PLUS (GE Healthcare) and stained for surface and intracellular markers. Permeabilization was performed using the Intracellular Fixation/Permeabilization Concentrate and Diluent kit (ThermoFisher). Antibodies and clones are described in Key resources table. Antibodies against CD8 and CD3 were conjugated to QDot 565 and 585 (Fisher), respectively. Cells were resuspended in 1% para-formaldehyde until acquisition on a BD Biosciences LSR II or a BD Symphony A5 cytometer. Fluorescence-minus-one controls were performed in pilot studies. DiOC6 (Fisher) staining was performed according to manufacturer instructions.

Co-culture experiments

Fresh PBMC were sorted for T cell subsets (Naive, $CD4^+CD45RA^+CD27^+$; $CXCR5^-$ memory, non-naive $CD4^+CXCR5^-$; cTfh, non-naive $CD4^+CXCR5^+PD\text{-}1^+$) or naive B cells $CD3^-CD19^+CD27^{lo}IgD^{hi}$. For each co-culture condition, $4.5x10^4$ sorted T cells were combined with autologous $5x10^4$ naive B cells. Co-cultures were either left unstimulated, stimulated with Staphyloccocal Enterotoxin B (SEB, Toxin Technologies, 0.5 μg/mL), SEB (0.5 μg/mL) with human TNF cytokine (Biolegend, 125 ng/mL), or SEB (0.5 μg/mL) with α-TNF antibodies (BD Biosciences, clone MAb11, 2 μg/mL). At the conclusion of the co-culture, supernatant was aspirated and saved. The remaining cells underwent anti-human Fc-blockade (Biolegend, TruStain FcX) for 10 minutes at room temperature, followed by routine staining for flow cytometry. The inhibitor of TNF processing TAPI-0 (Enzo, BML-PI133-0001) was used in Figure S3D. Cultures with B cells only were stimulated using soluble αIgM (10 ug/mL, clone DA4-4, Fisher) with soluble trimeric MegaCD40L protein (100 ng/mL, Enzo Life Sciences). For Figure S3E, samples were taken from previously-reported co-cultures[38] involving $CD4^+CXCR5^+PD\text{-}1^+$ cTfh from young or elderly adults combined with common allogenic naive B cells from a young adult donor in a 1:1 ratio for one week with SEB stimulation.

Multiplex bead assays

Multiplex bead assays for plasma samples were performed in duplicate for TNF, CXCL11, and MIP1β from the MILLIPLEX MAP Human Cytokine/Chemokine Magnetic Bead Panel (Millipore Sigma). Co-culture supernatants were assayed in duplicate for IgG1 production using the Legendplex Human Immunoglobulin Isotyping Panel (Biolegend) and data acquired on a BD Symphony A5 cytometer, in accordance with manufacturer instructions.

Transcriptomic analyses

PBMC were sorted on a BD Aria II cell sorter, followed by total RNA extraction by RNeasy Micro Plus kit (QIAGEN) and polyA amplification with SMARTer Ultra-Low Input RNA kit v3 (Clontech) according to manufacturer instructions. Libraries were prepared using the Illumina Nextera XT Library Preparation kit and sequenced on an Illumina HiSeq 2000 using 100bp single-read format. FASTQ files were trimmed with Trimmomatic (version 0.32),[76] aligned using STAR (version 2.5.2a)[77] and normalized by PORT (https://github.com/itmat/Normalization/, version 0.8.5) against the GRCh38 reference assembly of the human genome. Variance-stabilizing transformation and differential expression were performed using DESeq2 (version 1.20.0)[78] based on genes with at least 20 counts in at least 25% of all libraries, using the R environment (version 3.5.0). Of the 84 resultant libraries, one sample was excluded from further analyses (Figures S1H and S1I). Plots were made by ggplot2 (version 2.2.1) and heatmaps using the ''inferno'' color-scheme from the ''viridis'' library. For differential expression analysis, genes were included if they had at least 20 counts in at least 25% of the samples. Samples from the same person (e.g., inter-subset comparisons or day 0-to-day 7 comparisons) were treated as paired in statistical models for DESeq2. t-SNE maps were produced using Rtsne (version 0.13) from the transformed counts data. Gene set enrichment analyses[47] were performed with at least 10000 permutations of pre-ranked GSEA (https://www.gsea-msigdb.org/gsea/downloads.jsp). Gene ontology was performed in Cytoscape using ClueGo[80,81] or Metascape (https://metascape.org/gp/index.html#/main/step1).[82] Ingenuity Pathway Analysis (QIAGEN) was performed by uploading tables of the differential expression results from DESeq2

analyses for log_2 fold-change, p values, and p-adjusted values, followed by Expression Analysis core analysis for all genes with p value < 0.10. Upstream Regulator Analysis was used to calculate Z-scores in Figure 2G.[53,54] A potential regulator (drug, transcription factor, miRNA, etc) is associated with "activation" or "inhibition" effects on a series of downstream genes.[54] These associations are together summarized as a Z-score, in comparison to a model that assigns random regulation direction.

Network analysis

Weighted gene correlation network analysis (WGCNA, version 1.63)[51] was performed on variance-stabilizing transformation data, as calculated by DESeq2[78] after filtering out genes with less than 5 counts in fewer than 12% of all libraries. Adjacency matrix was calculated using $\beta = 20$. Minimum module size was 100. Gene ontology was analyzed using Metascape[82] for all genes with a module membership of at least 0.8. Pre-ranked GSEA was performed using all genes ranked by membership for each module. Transcription factors were identified from a curated list[52] and displayed with functional association data overlaid from GeneMANIA.[83]

Aging signature

Transcriptional profiling data for whole blood microarray studies was obtained from the Gene Expression Omnibus (GEO accession numbers 123697, 123696, and 123698), from Immport (SDY622, SDY648, SDY739, and SDY819), and from the European Genome-phenome Archive (EGAS00001002460). For each dataset, participants were stratified into cohorts for young adults (< 40 years old) or elderly adults (> 65 years old). Differential expression was calculated using GEO2R or by limma-voom.[79] An aging signature of 354 genes was constructed from genes downregulated in the elderly cohort from SDY739 with p.adj < 0.20 using limma-voom. For analyses of the aging signature in CD4 subsets, pre-ranked GSEA analyses were performed with at least 25000 permutations.

Influenza-specific antibodies

The two influenza A vaccine strains of the 2014/2015 seasonal influenza vaccine, A/California/7/2009 (H1N1) pdm09-like virus and A/Victoria/361/2011 (H3N2)-like virus, were obtained from the Centers for Disease Control and Prevention (Atlanta, GA). Assays to detect hemagglutinin inhibition assay (HAI) titers were performed. Infectious virus was used for neutralizing Ab assays or inactivated by β-propionolactone for H1N1/California- and H3N2/Victoria-specific binding Ab ELISA assays. Nunc Maxisorp plates (Nunc) were coated with 10 mg/mL influenza A/H1N1/California and A/H3N2/Victoria virus along with isotype standards for IgA1, IgG, and IgM (Athens Research and Technology) in bicarbonate buffer overnight at 4°C. Plates were blocked with 3% BSA in PBS and incubated with heat-inactivated sera of young and elderly adults. Abs were detected using alkaline phosphatase-conjugated mouse anti-human IgA1, IgG, and IgM (Southern Biotechnology).

QUANTIFICATION AND STATISTICAL ANALYSIS

Statistical analyses were performed with Prism 7 (GraphPad) and R. Data was compared using Student's t test, paired t test, one-way Analysis of Variance (ANOVA) with Tukey post hoc analysis, non-parametric ANOVA with Friedman's post-test, or Fisher's Exact test, as indicated. All t tests were performed as two-tailed tests at a 0.05 significance level. Outlier analysis for Figure 1E was performed using Grubb's test at $\alpha = 0.05$ and the plot with all points included is shown in Figure S1G. Study schematic in Figure 2A was diagramed using BioRender.

Cell Reports Medicine, Volume *2*

Supplemental information

Vaccine-induced ICOS^{+}CD38^{+} circulating Tfh are sensitive biosensors of age-related changes in inflammatory pathways

Ramin Sedaghat Herati, Luisa Victoria Silva, Laura A. Vella, Alexander Muselman, Cecile Alanio, Bertram Bengsch, Raj K. Kurupati, Senthil Kannan, Sasikanth Manne, Andrew V. Kossenkov, David H. Canaday, Susan A. Doyle, Hildegund C.J. Ertl, Kenneth E. Schmader, and E. John Wherry

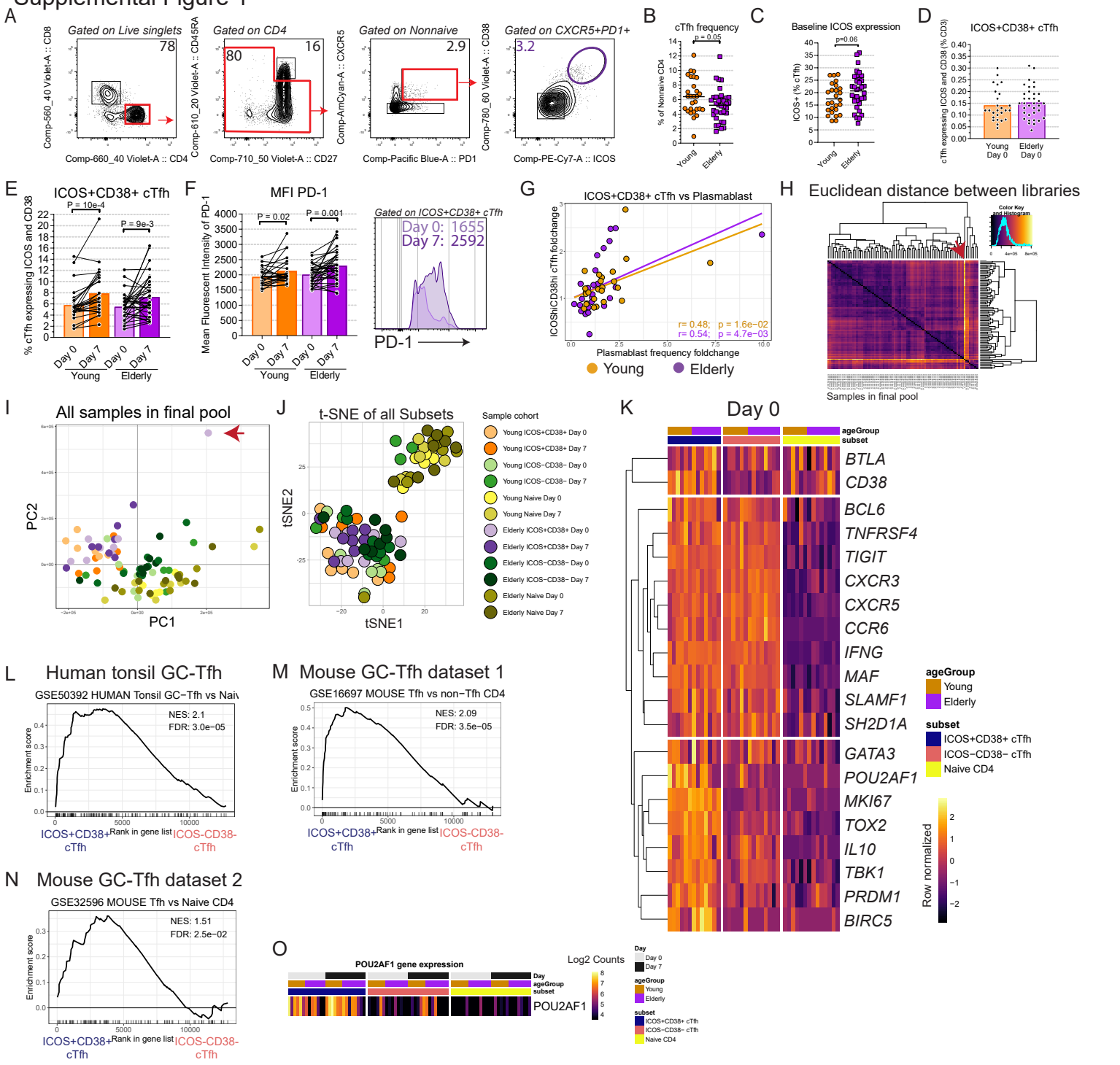

Supplemental Figure 1. Transcriptional profiling of circulating CD4 subsets. Related to Figure 1. **A**. Flow cytometry gating scheme shown for identifying cTfh subsets from peripheral blood. **B**. cTfh frequency shown as a proportion of nonnaive CD4 cells (P=0.05, t-test, n=28 young and n=35 elderly). **C**. Proportion of cTfh expressing ICOS (P=0.06, t-test, n=26 young and n=35 elderly). **D**. ICOS+CD38+ cTfh shown for young and elderly at baseline as a proportion of all CD3+ cells. **E**. Summary plots shown for frequency of cTfh co-expressing ICOS and CD38 for young (orange, $P=10^{-3}$, paired t-test, n=27) and elderly (purple, $P=8.6x10^{-3}$, paired t-test, n=35) at days 0 and 7 after vaccination. **F**. Summary plots shown for Mean Fluorescence Intensity of PD-1 (CD279) in ICOS+CD38+ cTfh for young (orange, P=0.015, paired t-test; n=27) and elderly (purple, $P=10^{-3}$; paired t-test; n=35) at days 0 and 7 after vaccination. Example PD-1 stain shown for one subject at day 0 (light purple) and 7 (dark purple) after influenza vaccination. Plot gated on ICOS+CD38+ cTfh. Geometric mean fluorescent intensity shown. **G**. Pearson correlation shown for the ICOS+CD38+ cTfh frequency fold-change from day 7 compared to day 0, vs the plasmablast response fold-change in frequency from day 7 compared to day 0. Shown is the full dataset with all outliers included for young (orange) and elderly (purple) subjects. **H**. Euclidean distance matrix calculated for all samples in the final pool for RNAseq after raw data processing. One outlier was identified by the red arrow and removed from further analysis. **I-J**. Principal component analysis (**I**) on all samples in the final pool for RNAseq after raw data processing. The outlier (same as in H) is indicated by arrow and was excluded from all subsequent analyses. t-Stochastic neighbor embedding (t-SNE) plot (**J**) showing the remaining 83 samples. **K**. Log-transformed transcriptional profiling data was queried for selected genes from the literature for young (orange bars) and elderly (purple bars) for CD4 subsets at day 0 after vaccination. Each column represents one unique subject. Heatmap is row-normalized. Row gaps and column gaps are based on hierarchical clustering and CD4 subsets, respectively. **L-N**. Normalized Enrichment Score (NES) and False Discovery Rate (FDR) q-value are shown for the pre-ranked gene set enrichment analysis (GSEA) comparison of ICOS+CD38+ cTfh to ICOS-CD38- cTfh at day 0 for all subjects combined, for GSE50392 (human tonsillar Tfh vs naïve CD4) (**L**), GSE16697 (mouse Tfh vs non-Tfh CD4) (**M**), and GSE32596 (mouse Tfh vs naïve CD4) (**N**). **O**. Log counts data shown for POU2AF1 for all samples in the final dataset.

Supplemental Figure 2

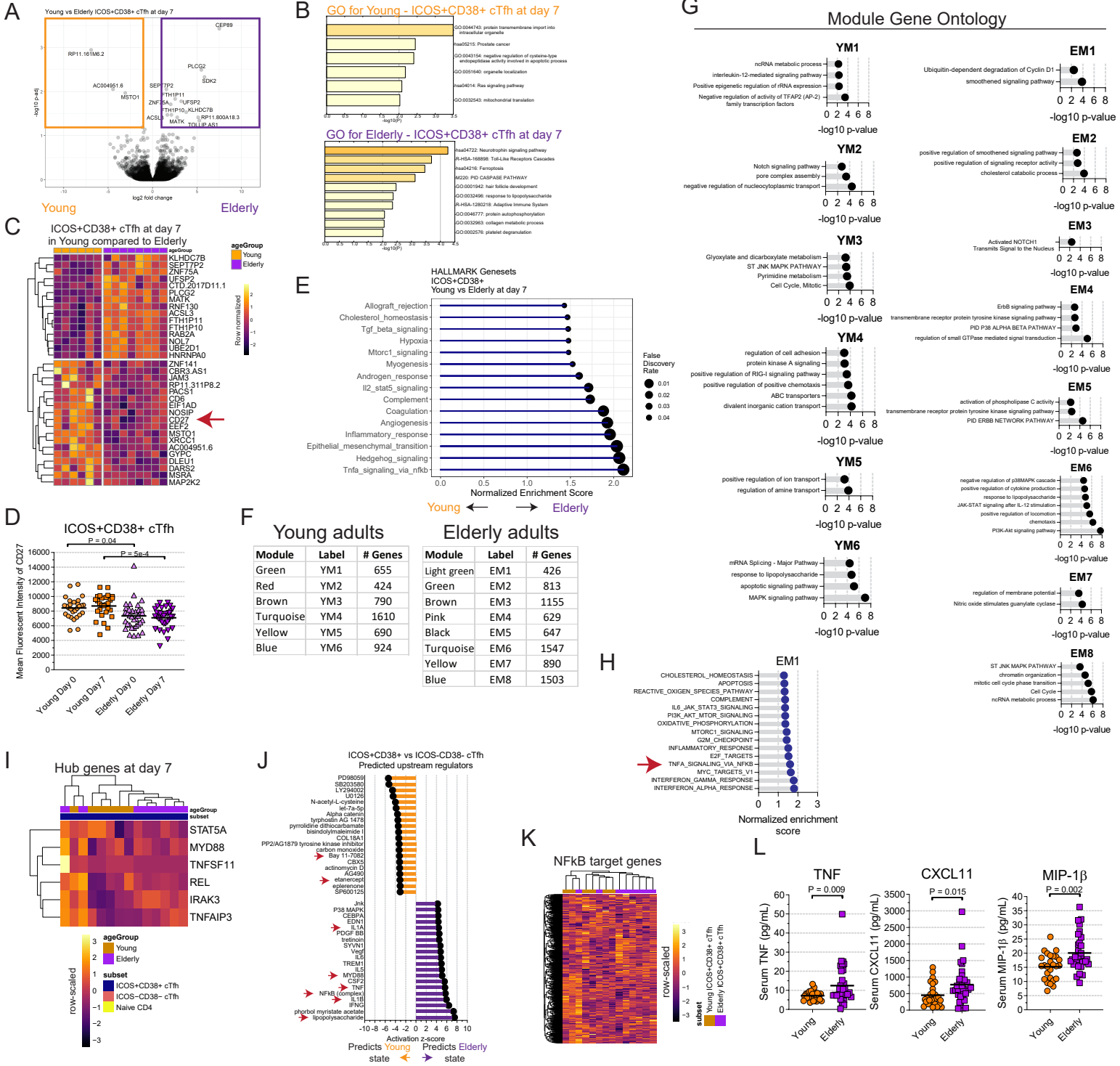

Supplemental Figure 2. Aging is associated with increased TNF-NFkB signaling in elderly. Related to Figure 2. **A**. Volcano plot for the differential expression analysis of ICOS+CD38+ cTfh from young adults and elderly adults at day 7 after vaccination. **B**. Gene ontology was performed on the 100 most differentially-expressed genes for ICOS+CD38+ cTfh at day 7 for young (middle) or elderly (bottom) subjects. **C**. Log-transformed transcriptional profiling data (left) was queried for differentially-expressed genes for the ICOS+CD38+ cTfh at day 7 from young (orange) and elderly (purple). Each column represents one unique subject. Heatmap is row-normalized and gaps are based on hierarchical clustering. **D**. Geometric mean fluorescence intensity of CD27 (right) is shown for the ICOS+CD38+ cTfh at days 0 and 7 (one-way ANOVA with Tukey's post-test; n=28 for young, n=35 for elderly). **E**. Pre-ranked GSEA was used to compare ICOS+CD38+ cTfh at day 7 from young vs elderly subjects. Pathways with FDR <0.05 shown. Positive NES indicate greater enrichment in the elderly than young. **F**. Weighted gene correlation network analysis was performed for ICOS+CD38+ cTfh at day 7 after vaccination for young adults and elderly adults separately. The six young adult modules and eight elderly adult modules were relabeled as indicated. **G**. Gene ontology by Metascape was performed for all genes in each module with module membership >0.80. **H**. Pre-ranked GSEA was performed on Elderly module EM1 using the Hallmark gene sets from MSigDB. TNF-NFkB gene set is indicated by the red arrow. **I**. Log_2-transformed gene counts as a row-normalized heatmap for ICOS+CD38+ cTfh at day 7 for the hub genes identified by network analysis. **J**. Ingenuity Pathway Analysis was used to assess predicted upstream regulators in the comparison of ICOS+CD38+ cTfh in young and elderly subjects at day 7 after vaccination. Top 20 highest and 20 lowest-scoring terms by activation z-score shown. Arrows indicate terms relevant to NFkB signaling. **K**. Gene targets of NFkB shown for ICOS+CD38+ cTfh at day 7 for young (orange) or elderly (purple) adults. Heatmap shows row-normalized log-transformed expression data for genes with nonzero variance. **L**. Plasma was profiled for inflammatory cytokines TNF, CXCL11, and MIP1β prior to vaccination.

Supplemental Figure 3

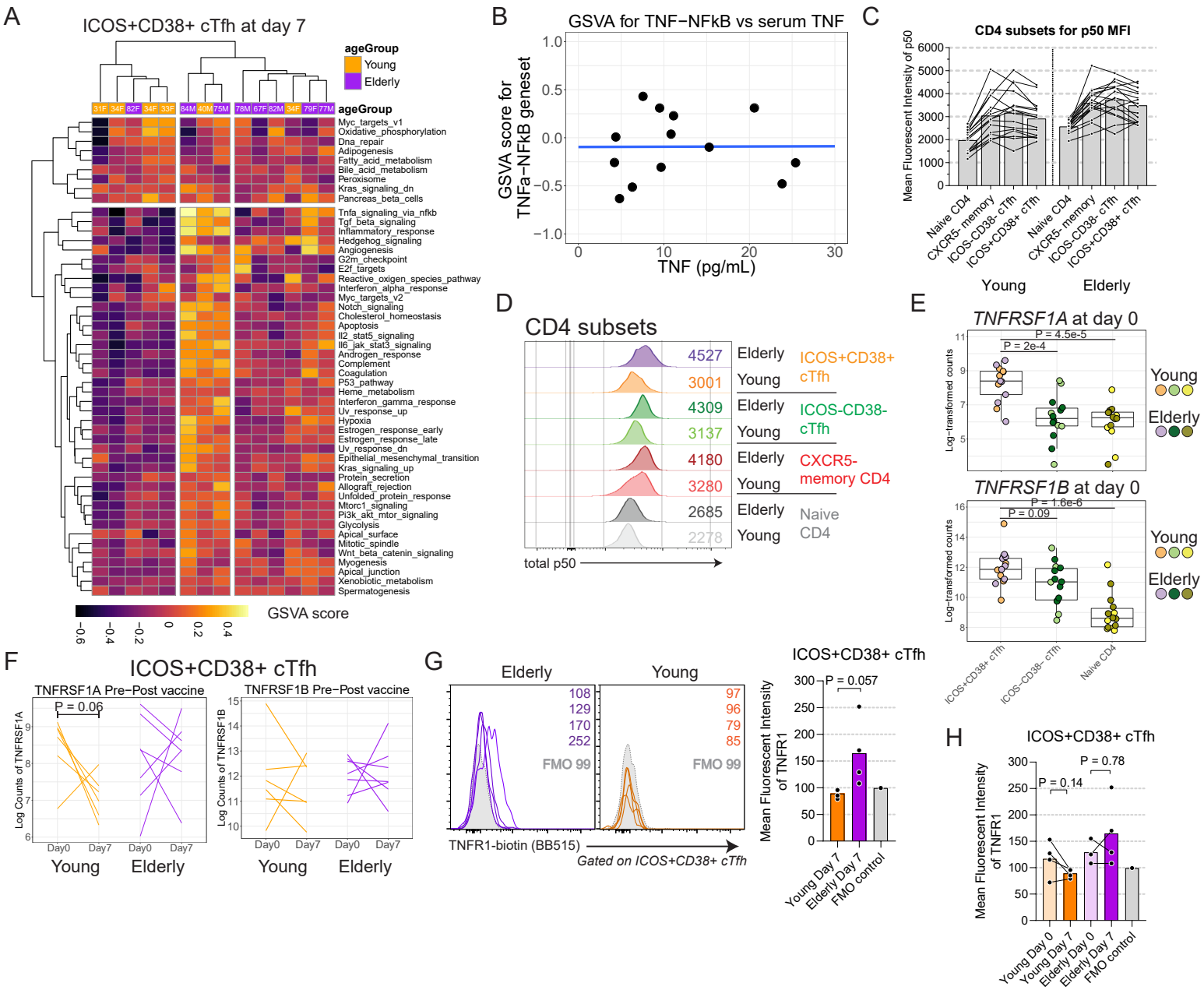

Supplemental Figure 3. Increased TNFR expression in cTfh. Related to Figure 2. A. Gene set variation analysis (GSVA) was performed for ICOS+CD38+ cTfh at day 7 from all 14 subjects for the Hallmark collection in MSigDB. Subject age and sex are shown. **B**. Scatter-plot shows GSVA score per subject compared to the plasma TNF concentration at baseline. **C-D**. PBMC were assayed by flow cytometry for total NFkB p50 protein expression. Numbers on histogram indicate mean fluorescence intensity for p50. Summary data and example plot shown for one young and one elderly subject for p50 protein in the different CD4 subsets. **E**. Log_2-transformed mRNA counts shown for gene expression for *TNFRSF1A* (left) or *TNFRSF1B* (right) in CD4 subsets for young and elderly subjects (one-way ANOVA with Tukey's, n=6 or 8). **f**. Gene expression of *TNFRSF1A* (left) and *TNFRSF1B* (right) were assessed from RNA-seq data, shown as before-and-after plots for normalized mRNA counts. Each line indicates one unique subject. **G**. TNFR1 protein was assessed by flow cytometry 7 days after influenza vaccination in an independent, randomly-selected subset of young and elderly adults from the same cohort. FMO control is shown in gray histogram on each plot. Summary plot is shown (P=0.057, t-test, n=3 for young and n=4 for elderly). **H**. Summary data for TNFR1 protein by flow cytometry is shown before and 7 days after vaccination for young (P=0.14, paired t-test, n=3) and elderly (P=0.78, paired t-test, n=3). Connected dots represent paired observations.

Supplemental Figure 4

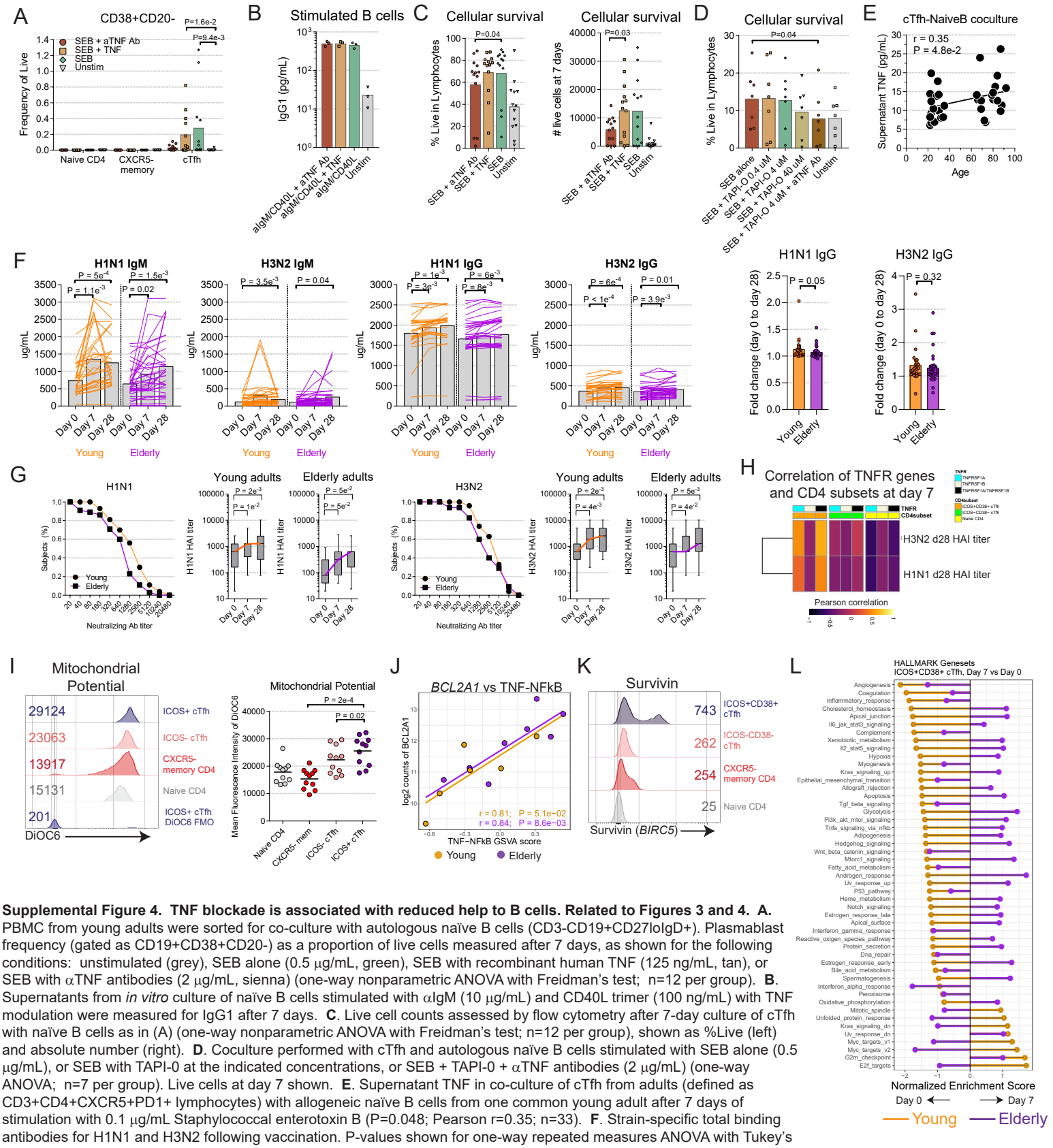

Supplemental Figure 4. TNF blockade is associated with reduced help to B cells. Related to Figures 3 and 4. A. PBMC from young adults were sorted for co-culture with autologous naïve B cells (CD3-CD19+CD27loIgD+). Plasmablast frequency (gated as CD19+CD38+CD20-) as a proportion of live cells measured after 7 days, as shown for the following conditions: unstimulated (grey), SEB alone (0.5 μg/mL, green), SEB with recombinant human TNF (125 ng/mL, tan), or SEB with αTNF antibodies (2 μg/mL, sienna) (one-way nonparametric ANOVA with Freidman's test; n=12 per group). **B.** Supernatants from *in vitro* culture of naïve B cells stimulated with αIgM (10 μg/mL) and CD40L trimer (100 ng/mL) with TNF modulation were measured for IgG1 after 7 days. **C.** Live cell counts assessed by flow cytometry after 7-day culture of cTfh with naïve B cells as in (A) (one-way nonparametric ANOVA with Freidman's test; n=12 per group), shown as %Live (left) and absolute number (right). **D.** Coculture performed with cTfh and autologous naïve B cells stimulated with SEB alone (0.5 μg/mL), or SEB with TAPI-0 at the indicated concentrations, or SEB + TAPI-0 + αTNF antibodies (2 μg/mL) (one-way ANOVA; n=7 per group). Live cells at day 7 shown. **E.** Supernatant TNF in co-culture of cTfh from adults (defined as CD3+CD4+CXCR5+PD1+ lymphocytes) with allogeneic naïve B cells from one common young adult after 7 days of stimulation with 0.1 μg/mL Staphylococcal enterotoxin B (P=0.048; Pearson r=0.35; n=33). **F.** Strain-specific total binding antibodies for H1N1 and H3N2 following vaccination. P-values shown for one-way repeated measures ANOVA with Tukey's post-test within each cohort. P-values for fold-change plots were calculated using Mann-Whitney U-test. **G.** Day 28 strain-specific neutralizing antibody titers as a cumulative distribution for H1N1 and H3N2 viral strains. Per-visit titers shown, with whiskers representing range and boxes representing the 25-75th percentiles. Line connects medians of each visit. P values calculated using repeated-measures ANOVA with Tukey's post-test. **H.** Pearson correlation for $\log_2$-transformed gene counts for TNFR genes as a heatmap for CD4 subsets against the neutralizing antibody response against each viral strain. **I.** Mitochondrial potential assessed with DiOC6. Example plot and summary data shown (one-way repeated-measures ANOVA with Tukey's; n=11 per group). **J.** Gene expression of *BCL2A1* from transcriptional profiling of ICOS+CD38+ cTfh at day 7 correlated against the GSVA scores for TNF-NFkB for young (orange, P=5.1x10^{-2}, Pearson r=0.81, n=6) and elderly (purple, P=8.6x10^{-3}, Pearson r=0.84, n=8). **K.** Flow cytometry for one young subject for Survivin protein. MFI shown. **L.** Aggregated GSEA results for the complete Hallmark gene sets collection for the comparison of day 7 vs day 0 for ICOS+CD38+ cTfh in young (orange) and elderly (purple). Positive enrichment scores indicate enrichment at day 7.

Supplemental Figure 5

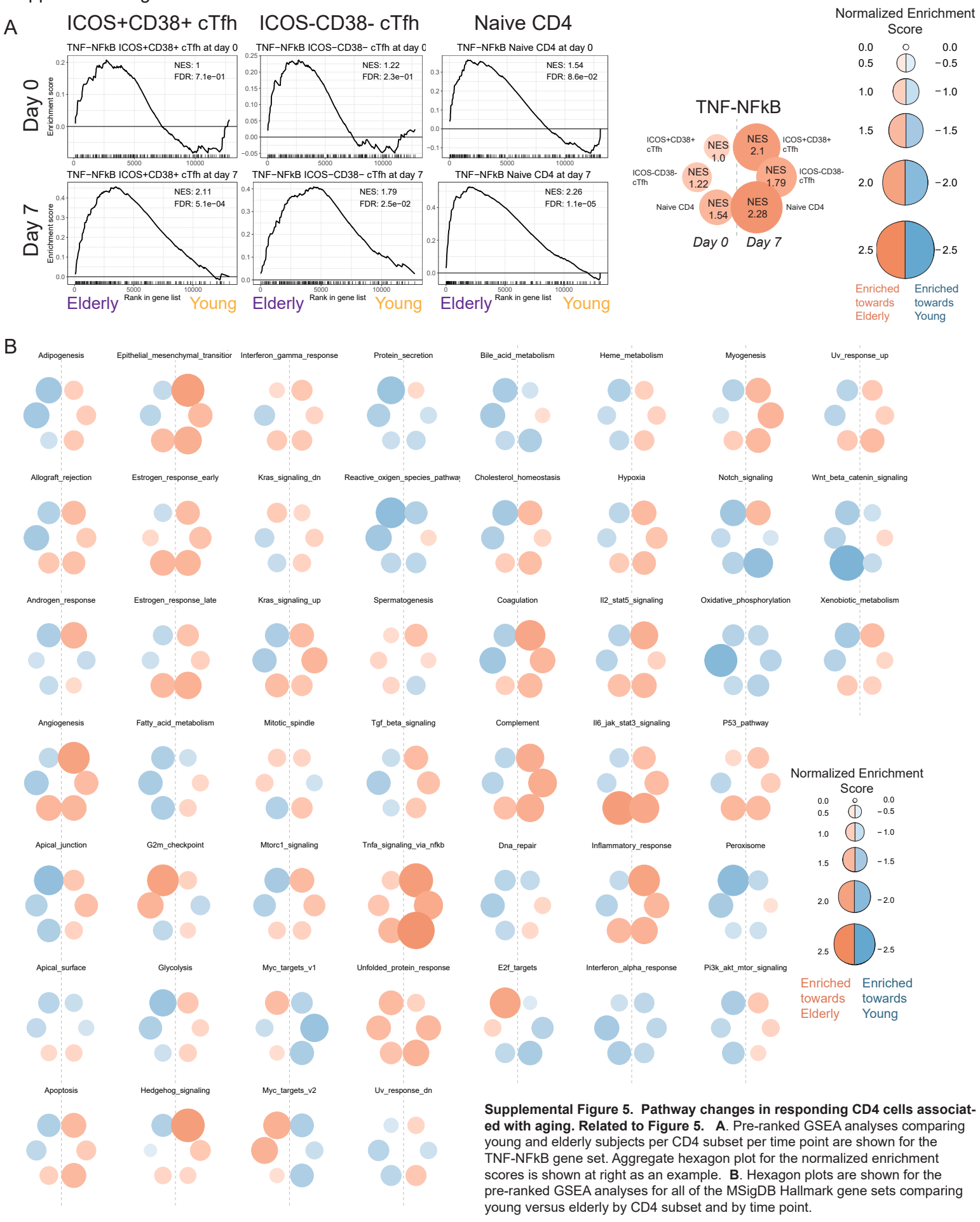

Supplemental Figure 5. Pathway changes in responding CD4 cells associated with aging. Related to Figure 5. **A**. Pre-ranked GSEA analyses comparing young and elderly subjects per CD4 subset per time point are shown for the TNF-NFkB gene set. Aggregate hexagon plot for the normalized enrichment scores is shown at right as an example. **B**. Hexagon plots are shown for the pre-ranked GSEA analyses for all of the MSigDB Hallmark gene sets comparing young versus elderly by CD4 subset and by time point.

Supplemental Figure 6

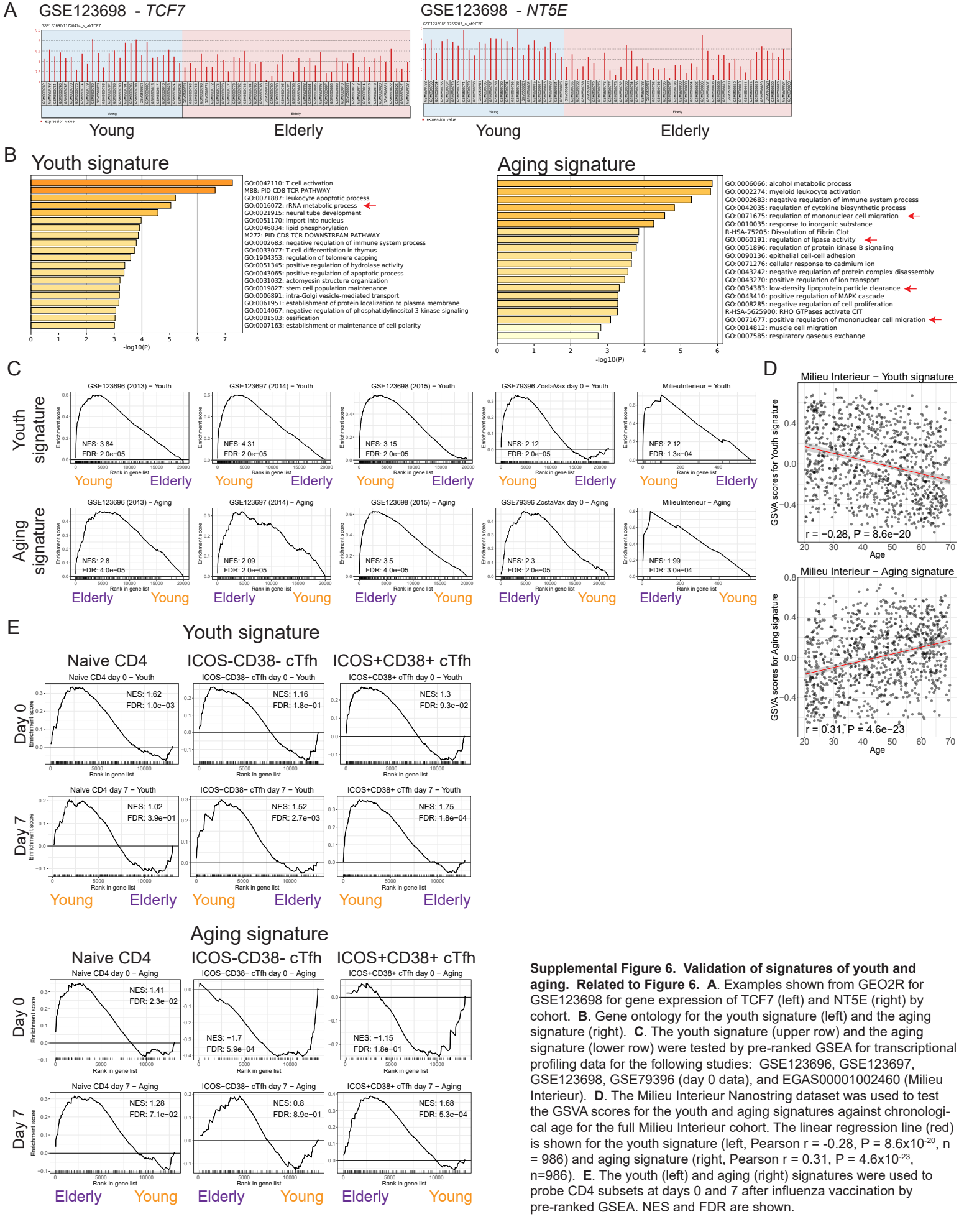

Supplemental Figure 6. Validation of signatures of youth and aging. Related to Figure 6. A. Examples shown from GEO2R for GSE123698 for gene expression of TCF7 (left) and NT5E (right) by cohort. **B**. Gene ontology for the youth signature (left) and the aging signature (right). **C**. The youth signature (upper row) and the aging signature (lower row) were tested by pre-ranked GSEA for transcriptional profiling data for the following studies: GSE123696, GSE123697, GSE123698, GSE79396 (day 0 data), and EGAS00001002460 (Milieu Interieur). **D**. The Milieu Interieur Nanostring dataset was used to test the GSVA scores for the youth and aging signatures against chronological age for the full Milieu Interieur cohort. The linear regression line (red) is shown for the youth signature (left, Pearson r = -0.28, P = 8.6×10^{-20}, n = 986) and aging signature (right, Pearson r = 0.31, P = 4.6×10^{-23}, n=986). **E**. The youth (left) and aging (right) signatures were used to probe CD4 subsets at days 0 and 7 after influenza vaccination by pre-ranked GSEA. NES and FDR are shown.

Supplementary Table 1. Clinical characteristics. Related to Figure 1

Cohort	Young (n=28)	Elderly (n=35)
Age		
Median	34	79
Mean (Standard deviation)	34.1 (2.59)	77.7 (4.93)
Range	30-40	66-85
Sex		
Male (%)	8 (29)	14 (40)
Race		
White	25 (89)	32 (91)
Black or African American	2 (7.1)	2 (5.7)
Other	1 (3.6)	1 (2.9)

Data are presented as number (% total) unless otherwise indicated.

Supplemental table 6: Whole-blood transcriptional profiling studies. Related to Figure 6.

StudyIdentifier	Young		Elderly		PMID Reference(s)	Weblink
	n	**range**	**n**	**range**		
SDY739	27	30-40	34	65-85	30186359, 27588486,	https://www.immport.org/shared/study/SDY739
	n	**range**	**n**	**range**		
GSE79396	33	25-40	44	60-79	28502771	https://www.ncbi.nlm.nih.gov/geo/query/acc.cgi?acc=GSE79396
GSE123696	17	23-34	49	66-96	30842675	https://www.ncbi.nlm.nih.gov/geo/query/acc.cgi?acc=GSE123696
GSE123697	25	23-32	35	67-97	30842675	https://www.ncbi.nlm.nih.gov/geo/query/acc.cgi?acc=GSE123697
GSE123698	26	24-36	42	68-97	30842675	https://www.ncbi.nlm.nih.gov/geo/query/acc.cgi?acc=GSE123698
Milieu Interieur	395	20-39	76	66-69	29282317, 25562703	https://www.ebi.ac.uk/ega/studies/EGAS00001002460
SDY622	27	30-40	35	65-88	30186359, 27588486,	https://www.immport.org/shared/study/SDY622
SDY648	28	30-40	33	65-87	30186359, 27588486,	https://www.immport.org/shared/study/SDY648
SDY819	15	30-40	30	65-89	30186359, 27588486,	https://www.immport.org/shared/study/SDY819